



## ORIGINAL ARTICLE

# Taxonomic revision of the *Tropicolotes nattereri* (Squamata, Gekkonidae) species complex, with the description of a new species from Israel, Jordan and Saudi Arabia

Marco Antônio Ribeiro-Júnior<sup>1</sup>  | Karin Tamar<sup>2</sup>  | Erez Maza<sup>1</sup> | Morris Flecks<sup>3</sup> | Philipp Wagner<sup>4</sup> | Boaz Shacham<sup>5</sup> | Marta Calvo<sup>6</sup> | Philippe Geniez<sup>7</sup> | Pierre-André Crochet<sup>8</sup> | Claudia Koch<sup>3</sup> | Shai Meiri<sup>1,2</sup>

<sup>1</sup>School of Zoology, Tel Aviv University, Tel Aviv, Israel

<sup>2</sup>The Steinhardt Museum of Natural History, Tel Aviv University, Tel Aviv, Israel

<sup>3</sup>Herpetology Section, Centre for Taxonomy and Morphology, Zoologisches Forschungsmuseum Alexander Koenig, Leibniz Institute for the Analysis of Biodiversity Change, Bonn, Germany

<sup>4</sup>Allwetterzoo Münster, Münster, Germany

<sup>5</sup>The National Natural History Collections, The Hebrew University of Jerusalem, Jerusalem, Israel

<sup>6</sup>Museo Nacional de Ciencias Naturales, Madrid, Spain

<sup>7</sup>Centre d'Ecologie Fonctionnelle et Evolutive, Univ Montpellier, CNRS, PSL-EPHE, IRD, Univ Paul Valéry Montpellier 3, Montpellier, France

<sup>8</sup>Centre d'Ecologie Fonctionnelle et Evolutive, Univ Montpellier, CNRS, EPHE, IRD, Univ Paul Valéry Montpellier 3, Montpellier, France

## Correspondence

Marco Antônio Ribeiro-Júnior, School of Zoology, Tel Aviv University, Tel Aviv 6997801, Israel.  
Email: majunior@gmail.com

## Funding information

This study was funded by: Gans Collections and Charitable Fund Inc., SYNTHESYS<sup>+</sup>, Synthesis of Systematic Resources funded by the European Commission [M.A.R.-J. grants: ES-TAF-1276; GB-TAF-2393; CZ-TAF-1260; DE-TAF-2418], the Rector scholarship, Tel Aviv University and the Alexander and Eva Lester Fund scholarship, I. Meier Segals Garden for Zoological Research.

## Abstract

We examined the taxonomy of the minute desert geckos of the *Tropicolotes nattereri* species complex using the largest morphological sampling, and the first molecular assessment of intraspecific diversity within this complex. We examined variation in mitochondrial and nuclear markers (*12S*, *ND2*, *c-mos* and *MC1R*) of 30 samples and analyzed the external morphology of 202 specimens, from across the entire distribution range of the complex from Egypt, Israel, Jordan and Saudi Arabia. We recognize two species under the name *T. nattereri*. We thus hereby describe a new species, *T. yomtovi* sp. n., and we redefine and redescribe *T. nattereri*, for which we designate a neotype. The species diversity in the genus *Tropicolotes* increases to 15.

## KEYWORDS

Middle East, Palearctic naked-toed geckos, reptiles, Saharo-Arabian reptiles, taxonomy

Ribeiro-Júnior and Tamar contributed equally to the work.

LSID urn:lsid:zoobank.org:pub:19BB9755-2B0E-4488-A49E-E8122A60FED2.

This is an open access article under the terms of the Creative Commons Attribution-NonCommercial-NoDerivs License, which permits use and distribution in any medium, provided the original work is properly cited, the use is non-commercial and no modifications or adaptations are made.

© 2022 The Authors. *Zoologica Scripta* published by John Wiley & Sons Ltd on behalf of Royal Swedish Academy of Sciences.

## 1 | INTRODUCTION

The gecko genus *Tropicolotes* Peters, 1880, comprises 14 species of minute lizards (smaller than 40-mm snout-vent length) with a Saharo-Arabian distribution pattern (Machado et al., 2021; Ribeiro-Júnior et al., 2022). Species of this genus are terrestrial, nocturnal and insectivorous members of the clade of Palearctic naked-toed geckos (Bauer et al., 2013). Although widely distributed, the genus is understudied and the species diversity and the taxonomy, of most of the currently recognized species, are far from being reliably known (Machado et al., 2021; Ribeiro-Júnior et al., 2022).

*Tropicolotes nattereri* Steindachner, 1901, was described based on two syntypes, one of them collected at 'Nawibi' (=Nuweiba, on the Eastern coast of the Sinai Peninsula, Egypt) and another at 'Bir al Mashiya' (=Bi'r al Mashi, on the Red Sea coast of Saudi Arabia), located on opposite sides of the Gulf of Aqaba (Red Sea). Steindachner (1901) described it as closely related to *T. steudneri*, differing from it by having larger eyes, slimmer body and longer limbs, with the hind limbs reaching the shoulder when pressed against body, and forelimbs reaching the nostril. However, even while presenting these characters as distinctive of the new species, Steindachner (1901) recognized that the hind limbs reaching the shoulder could represent a characteristic of the specimens rather than diagnostic features of the species. Since the original description, the syntypes of *T. nattereri* have not been mentioned in the taxonomic literature (Bauer & Günther, 1991). Many researchers studying the taxonomy of the genus *Tropicolotes* (ourselves included) have searched for them in European museums, including the Naturhistorisches Museum Wien, where Steindachner worked, but could not locate them. They are considered lost (Uetz et al., 2020). As a result, the species status of *T. nattereri* has been repeatedly questioned (Anderson, 1999; Arnold, 1977; Flowers, 1933; Guibé, 1966; Haas, 1951; Kluge, 1993; Loveridge, 1947; Minton et al., 1970). Baha El Din (1994) and Shifman et al. (1999), conducted comprehensive studies comparing specimens of *T. nattereri* from Sinai and Israel with specimens of *T. steudneri* from the African part of Egypt (west of the Suez Canal) and presented reliable results supporting differences between the two taxa.

The latest molecular phylogeny of the genus by Machado et al. (2021) included five specimens of *Tropicolotes nattereri* and presented the species as monophyletic and confined to the Levant. The same authors recognized two deeply diverged lineages within *T. nattereri*, here treated as the *T. nattereri* species complex. This complex is characterized by having unicarinate lamellae under the fingers and toes (Shifman et al., 1999; Ribeiro-Júnior

et al., 2022). We present here the results of a comprehensive revision of this complex, using molecular and morphological analyses.

## 2 | MATERIALS AND METHODS

### 2.1 | Molecular sampling and analyses

In order to evaluate genetic variability and estimate phylogenetic relationships within the *Tropicolotes nattereri* species complex, we constructed a dataset of 70 specimens of *Tropicolotes*. The phylogenetic dataset included specimens of most *Tropicolotes* species, apart from *T. chirioi*, *T. hormozganensis*, *T. tassiliensis* and *T. wolfgangboehmei* for which no complementary genetic sequences are available. We included 30 specimens of the *T. nattereri* species complex from across its distribution range, mainly from Israel with additional samples from Jordan and the Sinai Peninsula. We retrieved 40 sequences of other *Tropicolotes* species from GenBank (Machado et al., 2019, 2021; Metallinou et al., 2012). The monophyly of *Tropicolotes* has recently been established (Machado et al., 2019), and we therefore included one specimen of the phylogenetically closely related species, *Trachydactylus hajarensis*, as outgroup. Sample codes, voucher codes, localities and GenBank accession numbers are given in Table 1.

We extracted DNA from ethanol-preserved tissue samples using the Qiagen DNeasy Blood & Tissue Kit following the manufacturer's protocol. We amplified and bidirectionally sequenced two mitochondrial and two nuclear gene fragments for each individual respectively: the noncoding ribosomal 12S rRNA (*12S*; 423 bp), the protein-coding NADH dehydrogenase subunit 2 (*ND2*; 1039 bp), oocyte maturation factor *MOS* (*c-mos*; 393 bp) and melanocortin 1-receptor (*MC1R*; 666 bp). These markers were chosen because they were used in previous phylogenetic and taxonomic studies on *Tropicolotes* (Machado et al., 2019, 2021) and thus provide reliable and consistent comparison of phylogenetic relationships. We used the primers, polymerase chain reaction (PCR) conditions and source references as detailed in Machado et al. (2021). PCR products were purified with ExoSAP-IT™ PCR Product Cleanup Reagent (USB Europe GmbH, Stauf, Germany) and sequenced using ABI 3500xl Genetic Analyzer (Applied Biosystems). We checked, assembled and edited chromatographs using Geneious v.7.1.9 (Biomatter Ltd; Kearse et al., 2012). We aligned sequences, for each gene independently, using the online application of MAFFT v.7.3 (Katoh & Standley, 2013) with default parameters, except for the *12S* fragments to which we applied the Q-INS-I strategy that considers the secondary structure of RNA. Protein-coding genes were

TABLE 1 Information on the samples used in the phylogenetic analyses and their related GenBank accession numbers

Species (lineage)	Sample Code	Voucher Code	Country	Latitude	Longitude	I2S	ND2	CMOS	MCIR
<i>Tropicolotes algericus</i>	AP887		Morocco	28.890	-9.777	MT802848	MT802917	MT802944	MT802980
<i>Tropicolotes algericus</i>	BD7223		Morocco	27.156	-10.847	MT802847	MT802916	MT802943	MT802979
<i>Tropicolotes algericus</i>	MT6	BEV.10860	W. Sahara	25.774	-14.602	KC190710	MG990923	KC191023	MG990852
<i>Tropicolotes algericus</i>	MT5	BEV.10862	W. Sahara	23.568	-15.653	KC190709	MG990924		MG990853
<i>Tropicolotes bisharicus</i>	SPM002943(74)		Egypt	22.658	-35.332	MG990745	MG990925	MG990767	MG990854
<i>Tropicolotes confusus</i>	MCCIR.1609	MCCIR.1609	Oman	17.265	53.900	MG990751	MT802918	MG990776	MG990860
<i>Tropicolotes confusus</i>	MCCIR.1610	MCCIR.1610	Oman	17.113	54.713	MG990749	MT802921	MG990774	MG990858
<i>Tropicolotes confusus</i>	MCCIR.1777	MCCIR.1777	Oman	17.113	54.713	MG990750	MT802922	MG990775	MG990859
<i>Tropicolotes confusus</i>	OM113	NMP6V 74272/2	Oman	16.879	53.774	MG990747	MT802919	MG990772	MG990856
<i>Tropicolotes confusus</i>	OM114	NMP6V 74272/1	Oman	16.879	53.774	MG990748	MT802920	MG990773	MG990857
<i>Tropicolotes confusus</i>	TMHC406	NMP6V75045	Oman	16.884	53.773	MG990746	MG990926	MG990768	MG990855
<i>Tropicolotes nattereri</i> (A)	BEV.8860	BEV.8860	Israel	29.694	34.867	MT802858		MT802950	
<i>Tropicolotes nattereri</i> (A)	TAU.R.19698	TAU.R.19698	Israel	29.898	35.049	<b>OL998685</b>	<b>OL998708</b>	<b>OL998640</b>	<b>OL998663</b>
<i>Tropicolotes nattereri</i> (A)	TAU.R.19699	TAU.R.19699	Israel	29.898	35.049	<b>OL998686</b>	<b>OL998709</b>	<b>OL998641</b>	<b>OL998664</b>
<i>Tropicolotes nattereri</i> (A)	TAU.R.19700	TAU.R.19700	Israel	29.898	35.049	<b>OL998687</b>	<b>OL998710</b>	<b>OL998639</b>	<b>OL998665</b>
<i>Tropicolotes nattereri</i> (A)	ZFMK70653	ZFMK70653	Egypt	27.741	34.234	<b>OL998689</b>			
<i>Tropicolotes nattereri</i> (A)	ZFMK70657	ZFMK70657	Egypt	27.741	34.234	<b>OL998690</b>			
<i>Tropicolotes naybandensis</i>	ZFMK92345	ZFMK92345	Iran	27.333	52.658	MG990752	MG990928	MG990769	MG990862
<i>Tropicolotes naybandensis</i>	ZFMK92347	ZFMK92347	Iran	27.333	52.658	MT802860	MT802924	MT802951	MT802985
<i>Tropicolotes naybandensis</i>	ZFMK92344	ZFMK92344	Iran	27.333	52.658	MT802859			
<i>Tropicolotes nubicus</i>	BEV.9022	BEV.9022	Egypt	22.362	31.604	MT802869	MT802925	MT802954	MT802988
<i>Tropicolotes nubicus</i>	MT9	BEV.9020	Egypt	22.36	31.62	KC190706	MG990929	KC191021	MG990863
<i>Tropicolotes scortecii</i>	CN3485	IBECN3485	Oman	17.240	53.894	MG990758	MT802926	MG990782	MG990869
<i>Tropicolotes scortecii</i>	CN8984	IBECN8984	Oman	17.508	55.97	MG990763	MG990930	MG990770	MG990874
<i>Tropicolotes scortecii</i>	JEM108		Yemen	15.259	48.321	MG990753		MG990777	MG990864
<i>Tropicolotes scortecii</i>	JEM92		Yemen	15.164	51.032	MG990754		MG990778	MG990865
<i>Tropicolotes scortecii</i>	JIR103	NMP6V74788	Oman	17.933	55.527	MG990762	MT802928	MG990786	MG990873
<i>Tropicolotes scortecii</i>	TMHC399	NMP6V75042	Oman	17.683	54.262	MG990760	MT802927	MG990784	MG990871
<i>Tropicolotes somalicus</i>	TMHC455		Somalia	10.241	45.085	MG990765	MG990931	MG990771	MG990877
<i>Tropicolotes steudneri</i>	SPM002978(13)		Egypt	22.35	36.31	MT802890	MT802932	MT802960	
<i>Tropicolotes steudneri</i>	AP5860		Egypt	29.341	32.839	MT802876	MT802930	MT802955	MT802989

(Continues)

TABLE 1 (Continued)

Species (lineage)	Sample Code	Voucher Code	Country	Latitude	Longitude	I2S	ND2	CMOS	MCIR
<i>Tropicololotes steudneri</i>	MT10	BEV.10367	Egypt	25.324	34.744	KC190705	MG990932	KC191020	MG990878
<i>Tropicololotes steudneri</i>	AP5868		Egypt	29.072	32.447	MT802873	MT802929		
<i>Tropicololotes steudneri</i>	SPM002366 (73)		Egypt	24.66	35.1	MT802885	MT802931		
<i>Tropicololotes tripolitanus</i> (A)	BEV.9160	BEV.9160	Morocco	21.002	-13.150	MT802893		MT802961	MT802994
<i>Tropicololotes tripolitanus</i> (A)	BEV.9382	BEV.9382	Mauritania	20.438	-12.752	MT802895	MT802933	MT802962	MT802995
<i>Tropicololotes tripolitanus</i> (A)	MT7	BEV.10863	W. Sahara	22.571	-14.354	KC190711	MG990934	KC191024	MG990880
<i>Tropicololotes tripolitanus</i> (B)	BD2941		Mauritania	19.488	-13.063	MT802899	MT802935	MT802966	MT802999
<i>Tropicololotes tripolitanus</i> (B)	BD3524		Mauritania	19.462	-16.070	MT802900	MT802936	MT802967	MT803000
<i>Tropicololotes tripolitanus</i> (B)	BD4854		Mauritania	16.592	-12.144	MT802897	MT802934	MT802964	MT802997
<i>Tropicololotes tripolitanus</i> (B)	BD9658		Mauritania	16.710	-7.383	MT802906	MT802939	MT802970	
<i>Tropicololotes tripolitanus</i> (B)	IBES8156	IBES8156	Tunisia	33	9.376	MT802907	MT802940	MT802971	
<i>Tropicololotes tripolitanus</i> (B)	BD4981		Mauritania	17.212	-13.840	MT802902	MT802937	MT802968	MT803001
<i>Tropicololotes tripolitanus</i> (B)	BD9404		Mali	15.212	-11.628	MT802904	MT802938	MT802969	MT803002
<i>Tropicololotes tripolitanus</i> (B)	MT8	BEV.9025	Egypt	30.43	30.24	KC190712	MG990933	MT802977	MG990879
<i>Tropicololotes tripolitanus</i> (B)	BEV.10428	BEV.10428	Tunisia	32.908	9.7525	MT802908	MT802941		
<i>Tropicololotes yomtovi</i> sp. n. (B)	MT11	BEV.10886	Jordan	29.686	35.426	KC190708	MG990927	MT802949	MG990861
(Paratype)									
<i>Tropicololotes yomtovi</i> sp. n. (B)	TAU.R16538	TAU.R16538	Israel	29.574	34.972	OL998670	OL998694	OL998642	OL998656
<i>Tropicololotes yomtovi</i> sp. n. (B)	TAU.R19033	TAU.R19033	Israel	29.57	34.96	OL998677	OL998700	OL998643	OL998659
(Paratype)									
<i>Tropicololotes yomtovi</i> sp. n. (B)	TAU.R19032	TAU.R19032	Israel	29.57	34.96	OL998676	OL998699		
(Holotype)									
<i>Tropicololotes yomtovi</i> sp. n. (B)	TAU.R19042	TAU.R19042	Israel	29.57	34.96	OL998683	OL998706		
<i>Tropicololotes yomtovi</i> sp. n. (C)	BEV.8861	BEV.8861	Israel	31.464	35.393	MT802857	MT802948	MT802984	
<i>Tropicololotes yomtovi</i> sp. n. (C)	TAU.R16183	TAU.R16183	Israel	31.458	35.386	OL998669	OL998693	OL998647	OL998655
<i>Tropicololotes yomtovi</i> sp. n. (C)	TAU.R17469	TAU.R17469	Israel	31.348	35.364	OL998673	OL998697	OL998648	OL998658
<i>Tropicololotes yomtovi</i> sp. n. (C)	TAU.R19094	TAU.R19094	Israel	31.799	35.452	OL998684	OL998707	OL998650	OL998662
<i>Tropicololotes yomtovi</i> sp. n. (C)	TAU.R17855	TAU.R17855	Israel	30.937	35.38	OL998674			
<i>Tropicololotes yomtovi</i> sp. n. (C)	TAU.R17863	TAU.R17863	Israel	31.403	35.385	OL998675	OL998698		
<i>Tropicololotes yomtovi</i> sp. n. (D)	BEV.10196	BEV.10196	Israel	30.624	34.838	MT802856	MT802923	MT802947	MT802983
<i>Tropicololotes yomtovi</i> sp. n. (D)	TAU.R16085	TAU.R16085	Israel	30.623	35.192	OL998667	OL998691	OL998645	OL998653
<i>Tropicololotes yomtovi</i> sp. n. (D)	TAU.R16093	TAU.R16093	Israel	31.152	35.248	OL998668	OL998692	OL998646	OL998654

TABLE 1 (Continued)

Species (lineage)	Sample Code	Voucher Code	Country	Latitude	Longitude	I2S	ND2	CMOS	MC1R
<i>Tropicolotes yomtovi</i> sp. n. (D)	TAU.R16677	TAU.R16677	Israel	30.854	35.0714	<b>OL998672</b>	<b>OL998696</b>	<b>OL998651</b>	<b>OL998657</b>
<i>Tropicolotes yomtovi</i> sp. n. (D)	TAU.R19034	TAU.R19034	Israel	30.821	34.74	<b>OL998678</b>	<b>OL998701</b>	<b>OL998652</b>	<b>OL998660</b>
<i>Tropicolotes yomtovi</i> sp. n. (D)	TAU.R19040	TAU.R19040	Israel	30.6489	34.5068	<b>OL998681</b>	<b>OL998704</b>	<b>OL998649</b>	<b>OL998661</b>
<i>Tropicolotes yomtovi</i> sp. n. (D)	TAU.R19701	TAU.R19701	Israel	30.2821	35.0582	<b>OL998688</b>	<b>OL998711</b>	<b>OL998644</b>	<b>OL998666</b>
<i>Tropicolotes yomtovi</i> sp. n. (D)	BEV.10195	BEV.10195	Israel	30.6242	34.8388	MT802855			MT802982
<i>Tropicolotes yomtovi</i> sp. n. (D)	BEV.8490	BEV.8490	Israel	30.8547	34.7694	MT802854			
<i>Tropicolotes yomtovi</i> sp. n. (D)	TAU.R16634	TAU.R16634	Israel	30.79	34.77	<b>OL998671</b>	<b>OL998695</b>		
<i>Tropicolotes yomtovi</i> sp. n. (D)	TAU.R19035	TAU.R19035	Israel	30.821	34.74	<b>OL998679</b>	<b>OL998702</b>		
<i>Tropicolotes yomtovi</i> sp. n. (D)	TAU.R19039	TAU.R19039	Israel	30.6489	34.5068	<b>OL998680</b>	<b>OL998703</b>		
<i>Tropicolotes yomtovi</i> sp. n. (D)	TAU.R19041	TAU.R19041	Israel	30.6489	34.5068	<b>OL998682</b>	<b>OL998705</b>		
<i>Trachydactylus hajarensis</i>	CM3853/CN2575		Oman	20.2995	58.7497	KT302086	MG990922	KT302126	MG990850

Note: Letters in parentheses at the end of the species' names denote lineages presented in Figure 1. Accession numbers of sequences generated in this study are in bold.

translated into amino acids, and no stop codons were detected. For the nuclear genes, we coded the heterozygous positions according to the IUPAC ambiguity codes and resolved these sites, for each gene independently, by using the PHASE 2.1.1 algorithm (Stephens & Donnelly, 2003; Stephens et al., 2001) implemented in DNASP v.6 (Rozas et al., 2017) with probability threshold = 0.7. For the phased nuclear genes, we evaluated the occurrence of recombination by using the Pairwise Homoplasmy Index (PhiTest; Bruen et al., 2006) implemented in SplitsTree v.4.14.4 (Huson & Bryant, 2006), and none was detected (*CMOS*,  $p = .58$ ; *MC1R*,  $p = .57$ ).

We concatenated the individual gene alignments for the phylogenetic analyses. We used jModelTest v.2.1.7 (Darriba et al., 2012) to select the best model of nucleotide substitution for each gene under the Bayesian information criterion (BIC) resulting in the GTR + G model for both mitochondrial markers and the HKY + G for the two nuclear markers. We performed phylogenetic analyses of the partitioned concatenated datasets (complete, mitochondrial and nuclear) and of the individual markers under maximum likelihood (ML) and Bayesian inference (BI) frameworks. We conducted ML analyses using RAxML v.8.1.2 (Stamatakis, 2006) as implemented in raxmlGUI v.1.5 (Silvestro & Michalak, 2012). The ML analyses were performed with the thorough bootstrap analysis setting, GTRGAMMA model of sequence evolution and 100 random addition replicates. Nodal support was assessed with 1000 bootstrap replicates. We conducted BI analyses using MrBayes v.3.2.6 (Ronquist et al., 2012) with nucleotide substitution model parameters unlinked across partitions. The different partitions were allowed to evolve at different rates. Two simultaneous parallel runs were performed with four chains per run for  $2 \times 10^6$  generations with sampling every 200 generations. We examined the standard deviation of the split frequencies between the two runs and the potential scale reduction factor (PSRF) diagnostic; convergence was assessed by confirming that all parameters had reached stationarity and had sufficient effective sample sizes ( $>200$ ) using Tracer v.1.6 (Rambaut et al., 2014). We conservatively discarded the first 25% of trees as burn-in. We calculated interspecific and intraspecific uncorrected  $p$ -distances with pairwise deletion for each mitochondrial fragment in MEGA X (Kumar et al., 2018). We explored patterns of intraspecific diversity and nuclear allele sharing within the *Tropicolotes nattereri* species complex by inferring statistical parsimony networks for the two individual nuclear phase genes with the program TCS v.1.21 (Clement et al., 2000; connection limit of 95%), consisting of all sampled specimens for each marker (Table 1). We used tcsBU (Múrias dos Santos et al., 2016) for visualization of the nuclear networks.

## 2.2 | External morphology (meristic characters, measurements and colouration pattern)

We examined 202 specimens of the *Tropicolotes nattereri* species complex from Egypt (Sinai), Israel, Jordan and Saudi Arabia, representing the largest sample ever analyzed of a single *Tropicolotes* species. Specimens are deposited in the following herpetological collections: the Steinhardt Museum of Natural History, Tel Aviv, Israel (TAU.R); the Hebrew University of Jerusalem, Jerusalem, Israel (HUJ); the American Museum of Natural History, New York, USA (AMNH); California Academy of Sciences, San Francisco, USA (CAS); the Field Museum of Natural History, Chicago, USA (FMNH); the Centre d'Ecologie Fonctionnelle et Evolutive, Montpellier, France (BEV); the Natural History Museum, London, UK (BMNH); the Národní Muzeum, Prague, Czech Republic (NMP6V); and the Zoological Research Museum Alexander Koenig, Bonn, Germany (ZFMK). The list of examined specimens is presented below (in type series) and in the Referred Specimens in the Table S1. Comparisons with other species of the genus are based on Ribeiro-Júnior et al. (2022).

The meristic characters are: dorsal scales, counted from the forelimbs to the hindlimb level; ventrals, from the forelimbs to the hindlimb level; scale rows around the midbody; interorbitals, scales across the interorbital region at level of the mid orbits; supralabials; infralabials; gular scales, from the postmentals to the mandibular level; lamellae under the fourth finger; and lamellae under the fourth toe. The measurements are: snout–vent length, from the tip of the snout to the border of the cloaca; axilla–groin length, from the posterior margin of the forelimb to the anterior margin of the hind limb; head depth, at the highest point dorsoventrally; head width, at the widest point; head length, from the tip of the snout to the anterior margin of the tympanic aperture; neck length, from the posterior margin of the tympanic aperture to the anterior margin of the forelimb; lower arm length; shank length; and tail length. All measurements were taken with digital callipers ( $\pm 0.01$  mm), and all scale counts and other nonmetric morphological characters were counted using a stereomicroscope. Sex was tentatively determined based on general morphology, e.g. prominent swelling at the base of the tail (adult males), and well-developed calcium sacs in the sides of the neck (adult females). Therefore, because sex was tentatively defined, we present it with an asterisk (\*), needing confirmation.

Quantitative morphological distinctness between specimens of the clades A and B–D was tested using the Student's *t* tests (meristic data), and analyses of covariance with snout–vent length as a covariate in analyses of all measurements (except tail length because of small sample size; measurements of only intact tails [not regenerated or cut] were

collected, but they were not used in statistical analyses). Because we repeatedly tested for interspecific differences with several morphological variables, *p* values were compared with adjusted alpha levels using the false discovery rate method (Benjamini & Hochberg, 1995). Specimens not included in the molecular analyses were included in a given group according to morphological similarities with specimens included in the phylogenetic analyses. We statistically tested whether similarities/differences were supported. Meristic characters and measurements were analyzed separately, but together when using the false discovery rate method to adjust alpha levels. Additionally, we performed two principal component analyses (PCA) with the groups of *Tropicolotes nattereri* delimited by molecular analyses and *T. steudneri* (the species of which *T. nattereri* was previously considered as senior synonym): one PCA including all examined specimens and all meristic characters; and another including all specimens and all measurements (except tail length). Statistical analyses were implemented in PAST v.3.26 software (Hammer et al., 2001).

Colouration in preservative was described on the basis of the neotype/holotype, and variations thereof on the basis of specimens deposited in the herpetological collections mentioned above. The distribution map was produced using QGIS Las Palmas (v.2.18.3; <http://www.qgis.org/es/site/>) and occurrence data of all specimens studied; geographical coordinates are given in WGS 1984 datum.

Description format of the new species follows Ribeiro-Júnior et al. (2022), including modifications in an attempt to create a standardization of the nomenclature of characters (e.g. internasals, rather than 'supranasals' and 'postrostrals', and nasals, instead of 'nasalia' or 'postnasals'). Standardization of the character nomenclature in taxonomic studies is essential to avoid overlapping characters and/or duplications of names in future systematic studies (see Ribeiro-Júnior, 2018).

## 3 | RESULTS

### 3.1 | Molecular analyses

The datasets of the *Tropicolotes nattereri* species complex and the remaining species of *Tropicolotes*, respectively, included 30 and 40 sequences of *12S*, 23 and 36 sequences of *ND2*, 18 and 35 sequences of *c-mos*, and 18 and 33 sequences of *MC1R* (*ND2*, *c-mos* and *MC1R* could not be reliably obtained from specimens from Sinai) (see Figures S1 and S2 for the individual gene trees). Both the ML and BI phylogenetic trees of the complete concatenated dataset recovered identical topologies with all nodes well-supported (Figure 1). Our phylogenetic analyses recovered

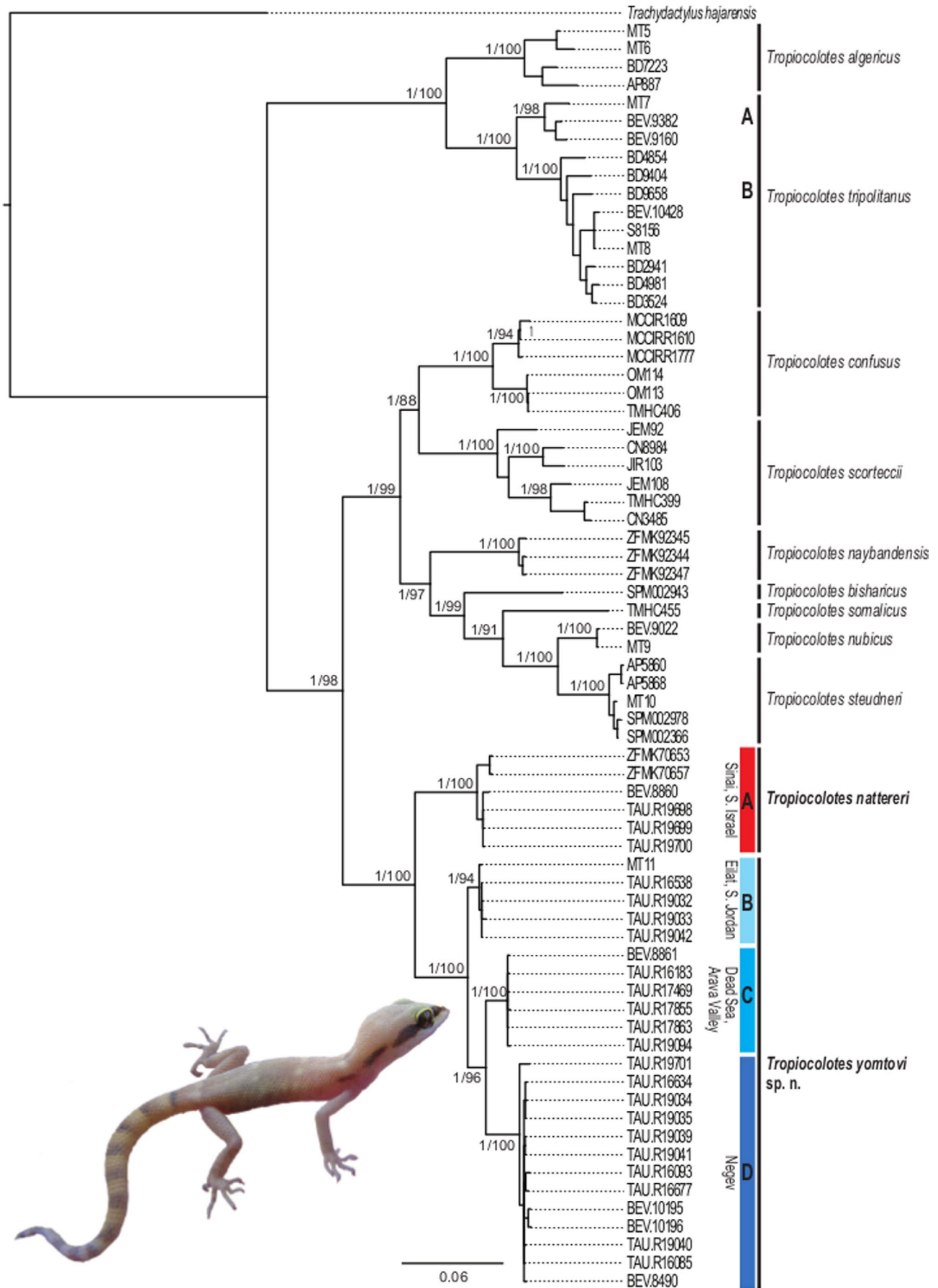


FIGURE 1 Bayesian inference phylogenetic tree of *Tropicolotes* based on the complete concatenated dataset (*12S*, *ND2*, *c-mos*, *MC1R*). Support values are indicated near the nodes (Bayesian posterior probabilities/ML bootstrap). Sample codes correlate with specimens in Table 1

two major clades, one of *T. algericus* and *T. tripolitanus* (with two subclades A and B for the latter species), and another one in which the *T. nattereri* species complex is monophyletic and sister to the remaining species. In both phylogenetic analyses, *T. nattereri* samples were divided into two clades with a total of four geographical lineages. One clade (clade A) includes specimens occurring in the Sinai Peninsula and southern Israel (from Eilat Mountains north to Yotvata) ( $n = 6$ ). The second clade (clades B–D) includes: (1) subclade B (Eilat and S. Jordan) occurring in southern Israel within and around the city of Eilat and southern Jordan ( $n = 5$ ); (2) subclade C (Dead Sea and Arava Valley) ranging along the western shores of the Dead Sea and northern Arava Valley, Israel ( $n = 6$ ); and (3) subclade D (Negev) distributed in the Negev Desert, Israel ( $n = 13$ ). According to the topologies of the concatenated datasets (Figures 1–2 and S3), clade A diverged first, followed by subclade B diverging from clades C and D.

The concatenated nuclear phylogenetic tree (Figure 2) recovered most species as monophyletic, with low support values for interspecific relationships. The four geographical lineages within the *Tropicolotes nattereri* species complex were also recovered as constituting a monophyletic group. The nuclear haplotype networks showed a structure similar to the two major clades recovered from the phylogenetic trees of the concatenated datasets, and a clear segregation of clade A and subclade B within the *T. nattereri* species complex, yet with subclades C–D sharing the same haplotype. The uncorrelated interspecific genetic distances among recognized species ranged between 6 and 19% in *12S* and 9 and 27% in *ND2* (Table 2). The lowest distances are between *Tropicolotes nubicus* and *T. steudneri* (6% in *12S* and 9% in *ND2*). The genetic divergences among the four geographical lineages within the *T. nattereri* species complex ranged between 2 and 9% in *12S* and 6 and 13% in *ND2*. The higher values represent distances between clade A and clades B–D: 7–9% in *12S* and 11–13% in *ND2*. Subclades B–D are separated by 2–4% in *12S* and 6–7% in *ND2* (Table 2). Therefore, based on the genetic distinctiveness of the *Tropicolotes* species (Machado et al., 2019, 2021), we considered two groups for the morphological analyses (clade A and clades B–D).

### 3.2 | Morphological analyses

Univariate statistical analyses (*t* test) revealed variable degrees of morphological divergence in meristic characters and ANCOVA in measurements between the two major clades (A and B–D) recognized in the *Tropicolotes nattereri* species complex by molecular analyses. Six of the

nine meristic characters and five of the nine measurements present significant differences between them (Table 3). Members of clade A have more interorbital scales, supralabials, infralabials, gular scales and lamellae under fourth fingers and toes, than members of clades B–D. Clade A members also have longer snout–vent length, axilla–groin length, head, lower arms and shanks. The absolute frequency, relative frequency and mean  $\pm$  standard error for each character are presented in Figure S4, and *p* values and significance based on the false discovery rate method are shown in Table S2.

Our multivariate analyses using nine meristic characters presented a complete separation between *Tropicolotes steudneri* and *T. nattereri* species group (Figure S5A), but the same analyses including all measurements (except tail length) failed to discriminate species (Figure S5B). The clades within the *T. nattereri* species complex failed to present a visual separation in either analysis. The first two components of the PCA using meristics explained 76.2% of the total variance in the characters (62.2% and 14.0% respectively), and the most important characters in the first component were dorsal and midbody scales and in the second component were gular and ventral scales. In the PCA considering seven measurements, the first two components explained 97% of the total variance in the characters (95.2% and 1.8% respectively), and the most important characters in the first and second components were snout–vent and axilla–groin lengths.

#### 3.2.1 | Taxonomic status of the two groups within *Tropicolotes nattereri*

Based on the original description of *Tropicolotes nattereri* Steindachner, 1901, the phylogenetic position of our samples from Sinai (Egypt; clade A) and morphological similarities of the specimens used in the molecular analyses with other specimens from the same region, we first decided which group is *T. nattereri* sensu stricto, and we redescribed this taxon. Specimens with molecular samples belonging to clades B–D are thus referred to as *Tropicolotes* sp. n. and then used for morphological comparisons with *T. nattereri*. Once morphological differences had been defined, we used them to identify the other specimens from the wide distribution of *T. nattereri* sensu lato. *Tropicolotes* sp. n. from Israel, Jordan, Sinai and Saudi Arabia is not conspecific with *T. nattereri* or with any previously recognized congener. Therefore, based on the overall congruence with lineages identified and species delimited in the molecular analyses, here we redefine and redescribe *T. nattereri*,



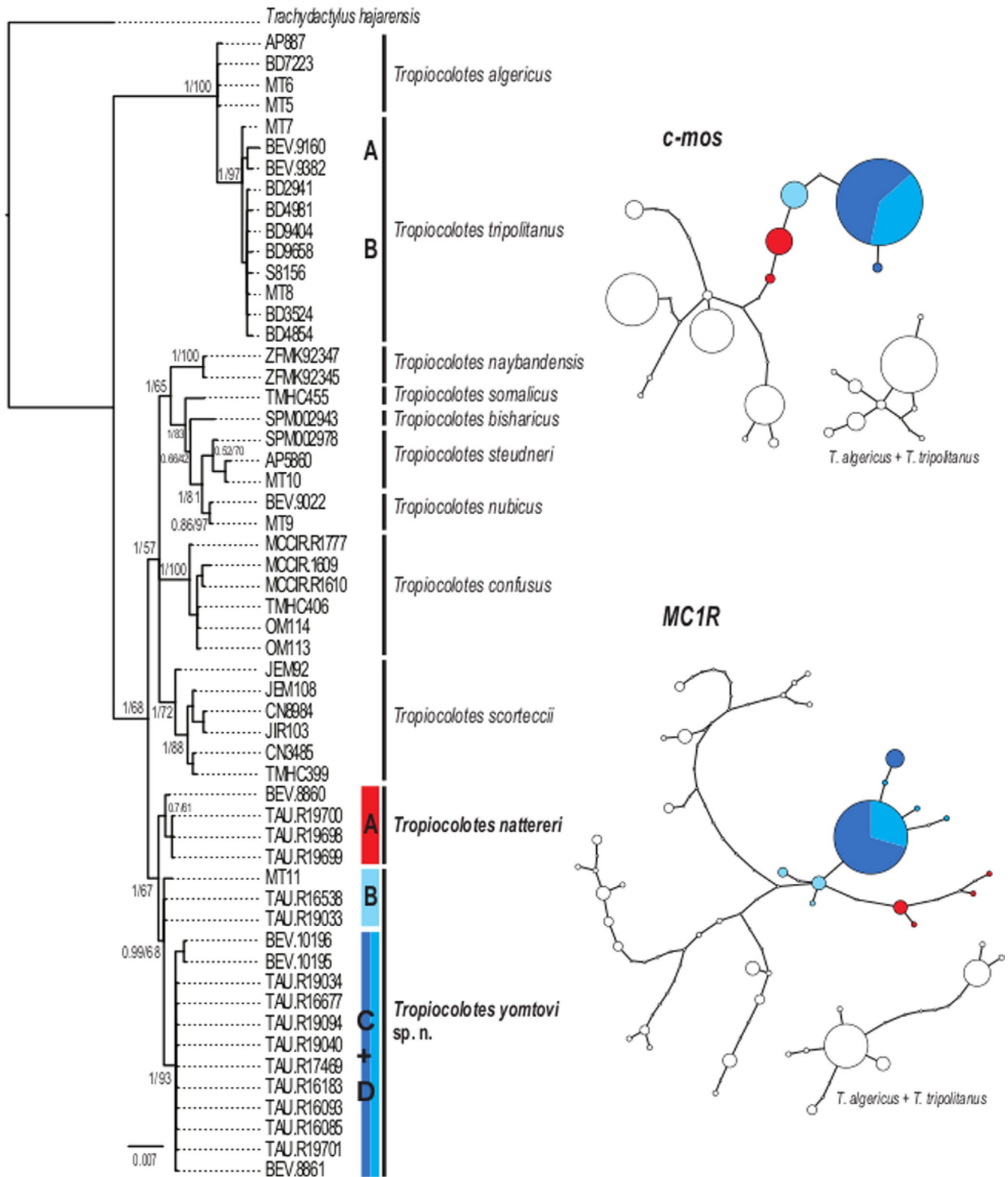


FIGURE 2 Phylogenetic relationships of *Tropicolotes* based on the nuclear dataset. Colours correspond to those in Figures 1 and 3. Left: Bayesian inference phylogenetic tree of the concatenated nuclear dataset (*c-mos* and *MC1R*). Support values are indicated near the nodes (Bayesian posterior probabilities/ML bootstrap). Sample codes correlate with specimens in Table 1. Right: Phylogenetic networks based on nuclear haplotypes for the *CMOS* (top) and *MC1R* (bottom) gene fragments. Circle size is proportional to the number of individuals. Colours refer to the *T. nattereri* species complex only

**TABLE 2** Pairwise uncorrected sequence divergence (*p*-distance) of *Tropicolotes* derived from the mitochondrial genes *12S* (below the diagonal) and *ND2* (above the diagonal). Letters in parentheses at the end of the species names denote lineages presented in Figure 1

Taxon (lineage)	1	2	3	4	5	6	7	8	9	10	11	12	13	14
1. <i>T. algericus</i>		0.24	0.25	0.24	0.26	0.22	0.25	0.26	0.25	0.16	0.16	0.23	0.23	0.25
2. <i>T. bisharicus</i>	0.16		0.16	0.20	0.17	0.15	0.19	0.16	0.17	0.23	0.25	0.19	0.20	0.21
3. <i>T. confusus</i>	0.16	0.12		0.19	0.17	0.17	0.16	0.19	0.19	0.24	0.25	0.19	0.21	0.22
4. <i>T. nattereri</i> (A)	0.13	0.13	0.12		0.20	0.18	0.19	0.21	0.23	0.23	0.23	0.11	0.13	0.13
5. <i>T. naybandensis</i>	0.17	0.09	0.09	0.13		0.15	0.19	0.18	0.19	0.24	0.25	0.19	0.20	0.21
6. <i>T. nubicus</i>	0.16	0.10	0.12	0.12	0.08		0.21	0.14	0.09	0.26	0.22	0.20	0.21	0.23
7. <i>T. scorteccii</i>	0.18	0.15	0.11	0.13	0.12	0.14		0.21	0.20	0.23	0.25	0.20	0.20	0.21
8. <i>T. somalicus</i>	0.17	0.09	0.14	0.14	0.11	0.09	0.15		0.17	0.26	0.27	0.20	0.21	0.23
9. <i>T. steudneri</i>	0.16	0.10	0.10	0.12	0.07	0.06	0.12	0.09		0.25	0.26	0.21	0.22	0.24
10. <i>T. tripolitanus</i> (A)	0.12	0.18	0.17	0.18	0.17	0.18	0.18	0.17	0.18		0.11	0.22	0.22	0.24
11. <i>T. tripolitanus</i> (B)	0.11	0.17	0.16	0.14	0.17	0.18	0.19	0.17	0.18	0.06		0.23	0.23	0.25
12. <i>T. yomtovi</i> sp. n. (B)	0.14	0.12	0.11	0.07	0.12	0.13	0.14	0.14	0.11	0.17	0.15		0.06	0.07
13. <i>T. yomtovi</i> sp. n. (C)	0.13	0.12	0.11	0.07	0.12	0.13	0.14	0.14	0.12	0.15	0.13	0.02		0.07
14. <i>T. yomtovi</i> sp. n. (D)	0.15	0.14	0.13	0.09	0.14	0.14	0.14	0.16	0.13	0.18	0.16	0.03	0.04	

including the designation of a neotype, and we present a second taxon new to science, *T. yomtovi* sp. n. that also features unicarinate lamellae under the fingers and toes. Zoobank registration for the new species: urn:lsid:zoobank.org:act:587DE30E-D73F-4EBA-97D1-534B006A8A1D. Below, we provide the redescription of *T. nattereri* and the description of *T. yomtovi* sp. n.. Figures of the type series and other representatives of each species, including plates presenting population variation in colour pattern, are included in Appendix S1. We discuss the systematic rank and nomenclatural status of these two lineages in the Discussion section.

Squamata Oppel, 1811

Gekkonidae Gray, 1825

*Tropicolotes* Peters, 1880

*Tropicolotes nattereri* Steindachner, 1901

(Figures 1–3; Tables 1–3; Figures S1–S7, and Table S1).

*Tropicolotes nattereri* Flowers (1933, in part); Loveridge (1947, in part); Schmidt and Marx (1956, in part); Werner (1973, in part); Baha El Din (1994, in part, Figure 1A–B); Shifman et al. (1999, in part, Figure 2A–B); Bouskila and Amitai (2001, in part); Sindaco and Jeremcenko (2008, in part); Wilms et al. (2010, in part); Bar and Haimovitch (2012, in part); Krause et al. (2013, in part); Werner (2016, in part); Bar and Haimovitch (2018, in part); Bar et al. (2021, in part).

*Tropicolotes nattereri* “B” Machado et al. (2021).

*Tropicolotes steudneri* Flowers (1933, in part); Loveridge (1947, in part); Schmidt and Marx (1956, in part); Werner (1973, in part); Arbel (1984, in part); Werner (1988, in part); Kluge (1993, in part); Baha El Din (1994, in part).

#### Neotype

TAU.R 12138, adult, female\*, collected on 21 February 1980 by Uri Marder, at Dahab, Eastern Sinai, Egypt (28.50° N, 34.51° E) (Figure S6).

#### Referred specimens

List of specimens in Table S1.

#### Diagnosis

*Tropicolotes nattereri* is distinguished from all other species of *Tropicolotes* by the combination of the following characters: (1) unicarinate lamellae under fingers and toes; (2) mean snout–vent length = 23.57 mm; (3) mean axilla–groin length = 10.45 mm; (4) mean head length = 6.63 mm; (5) mean lower arm length = 4.21 mm; (6) mean shank length = 5.00 mm; (7) mean number of interorbitals = 16.64; (8) mean number of supralabials = 9.62; (9) mean number of infralabials = 8.05; (10) mean number of gular scales = 33.51; (11) mean number of lamellae under fourth fingers = 13.51; and (12) mean number of lamellae under fourth toes = 17.03.

#### Comparison with other species

*Tropicolotes nattereri* differs from all other species of *Tropicolotes* (*T. algericus*, *T. bisharicus*, *T. chirioi*, *T. confusus*, *T. hormozganensis*, *T. naybandensis*, *T. nubicus*, *T. scorteccii*, *T. somalicus*, *T. steudneri*, *T. tassiliensis*, *T. tripolitanus apoklomag*, *T. tripolitanus occidentalis*, *T. tripolitanus tripolitanus* and *T. wolfgangboehmei*), except *T. yomtovi* sp. n. in having unicarinate lamellae under the fourth fingers and toes (vs. tricarinate lamellae). It differs from *T. yomtovi* sp. n. in having longer snout–vent

**TABLE 3** Summary of the variation in meristic characters, measurements (in mm) and body proportions in *Tropicolotes nattereri* (clade A) and *T. yomtovi* sp. n. (clades B–D)

<b>Meristics (<i>t</i> test)</b>	<b><i>T. nattereri</i> (<i>n</i> = 39)</b>	<b><i>T. yomtovi</i> sp. n. (<i>n</i> = 106)</b>
Dorsals	42–59	48–60
( <i>t</i> = 1.63; <i>p</i> = .105)	(52.97; 17.29)	(53.95; 7.58)
Ventrals	46–55	40–58
( <i>t</i> = 0.66; <i>p</i> = .509)	(50.13; 6.11)	(49.77; 8.88)
Midbody	43–53	42–55
( <i>t</i> = 1.96; <i>p</i> = .052)	(48.87; 7.75)	(47.85; 7.63)
Interorbitals*	14–19	13–17
( <i>t</i> = 6.51; <i>p</i> < .001)	(16.64; 1.32)	(15.31; 1.05)
Supralabials*	8–11	7–11
( <i>t</i> = 5.72; <i>p</i> < .001)	(9.62; 0.58)	(9.05; 0.52)
Infralabials*	7–10	7–9
( <i>t</i> = 4.67; <i>p</i> < .001)	(8.05; 0.35)	(7.69; 0.31)
Gulars*	28–39	25–37
( <i>t</i> = 3.44; <i>p</i> < .001)	(33.51; 6.15)	(31.98; 5.14)
Lamellae under 4th finger*	11–16	10–15
( <i>t</i> = 5.79; <i>p</i> < .001)	(13.51; 0.93)	(12.71; 1.14)
Lamellae under 4th toe*	15–19	13–20
( <i>t</i> = 4.52; <i>p</i> < .001)	(17.03; 1.09)	(16.24; 1.96)
<b>Measurements (ANCOVA, except SVL)</b>	<b><i>T. nattereri</i> (<i>n</i> = 32)</b>	<b><i>T. yomtovi</i> sp. n. (<i>n</i> = 156)</b>
Snout–vent length*	17.34–30.01	12.20–28.71
( <i>t</i> = 2.179; <i>p</i> = .031)	(23.57; 11.12)	(22.24; 9.11)
Axilla–groin length*	7.45–13.28	5.49–13.42
( <i>p</i> = .0001)	(10.45; 3.02)	(10.20; 2.81)
Head depth	1.97–3.56	1.55–3.79
( <i>p</i> = .779)	(2.78; 0.13)	(2.64; 0.18)
Head width	3.39–5.38	2.61–5.31
( <i>p</i> = .778)	(4.25; 0.26)	(4.08; 0.27)
Head length*	5.35–8.81	4.28–7.57
( <i>p</i> = .005)	(6.63; 0.66)	(6.17; 0.49)
Neck length	3.28–5.59	2.10–5.20
( <i>p</i> = .211)	(4.26; 0.45)	(3.96; 0.35)
Lower arm length*	3.30–5.50	2.12–4.61
( <i>p</i> < .0001)	(4.21; 0.30)	(3.56; 0.25)
Shank length*	3.81–6.17	2.61–5.52
( <i>p</i> < .0001)	(5.00; 0.42)	(4.24; 0.32)
Tail length	20.01–32.86	10.35–32.16
( <i>p</i> = .462)	( <i>n</i> = 15; 25.01; 15.53)	( <i>n</i> = 62; 23.32; 20.57)
<b>Body proportions</b>	<b><i>T. nattereri</i> (<i>n</i> = 32)</b>	<b><i>T. yomtovi</i> sp. n. (<i>n</i> = 156)</b>
Axilla–groin length/snout–vent length*	0.38–0.48	0.38–0.53
	(0.44 ± 0.02)	(0.46 ± 0.03)
Head length/snout–vent length*	0.26–0.31	0.24–0.36
	(0.27 ± 0.01)	(0.28 ± 0.02)

(Continues)

TABLE 3 (Continued)

Body proportions	<i>T. nattereri</i> (n = 32)	<i>T. yomtovi</i> sp. n. (n = 156)
Head width/snout–vent length	0.16–0.21 (0.18 ± 0.02)	0.15–0.22 (0.18 ± 0.01)
Head depth/snout–vent length	0.08–0.15 (0.12 ± 0.02)	0.09–0.17 (0.12 ± 0.01)
Neck length/snout–vent length	0.13–0.23 (0.18 ± 0.02)	0.13–0.24 (0.18 ± 0.02)
Lower arm length/snout–vent length*	0.15–0.22 (0.18 ± 0.02)	0.13–0.20 (0.16 ± 0.01)
Shank length/snout–vent length*	0.17–0.27 (0.21 ± 0.02)	0.16–0.23 (0.19 ± 0.01)

Note:  $n$  = total number of specimens studied; counts and measurements are presented as minimum–maximum (mean; standard error); significant differences (at  $\alpha = 0.05$ ) of  $t$  tests (meristics and snout–vent length) and ANCOVAs (all measurements except snout–vent length, in models using snout–vent length as a covariate) are marked with an asterisk. In tail length,  $n$  = number of intact tails measured.  $p$  values adjusted using the false discovery rate method are presented in Table S2.

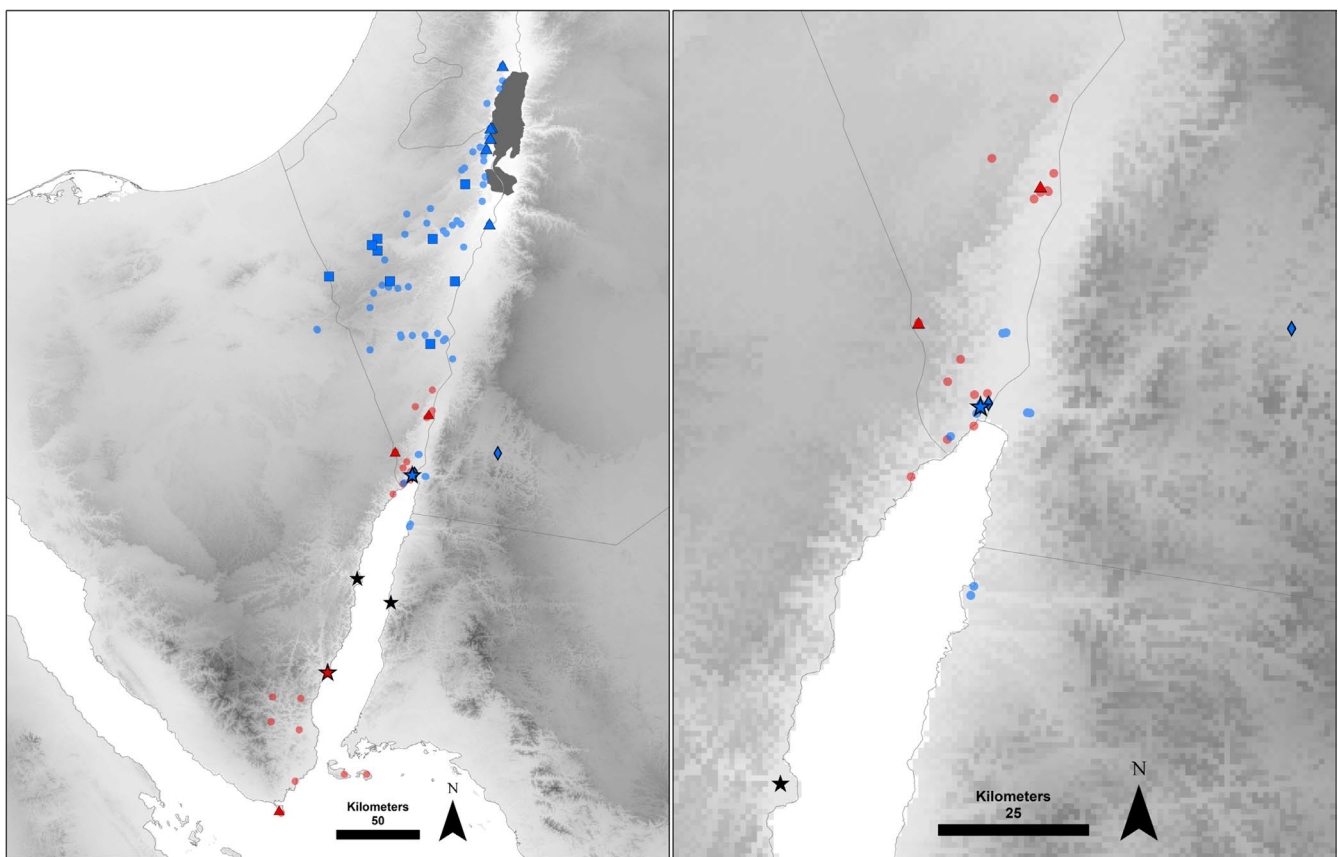


FIGURE 3 Distributional records of *Tropicolotes nattereri* (red) and *T. yomtovi* sp. n. (blue). Stars mark the type localities, including those of the syntypes of *T. nattereri* (Steindachner, 1901) (black stars). Larger symbols represent samples included in the molecular analyses (red triangles = subclade A; diamonds = subclade B; blue triangles = subclade C; squares = subclade D). Right: closer view of northern Gulf of Aqaba

(means = 23.57 mm vs. 22.24 mm), head (means = 6.63 mm, vs. 6.17 mm), axilla–groin (means = 10.45 mm, vs. 10.20 mm), lower arms (means = 4.21 mm, vs. 3.56 mm) and shanks (means = 5.00 mm, vs. 4.24 mm); higher

number of supralabials (means = 9.62, vs. 9.05), infralabials (means = 8.05, vs. 7.69), gulars (means = 33.51, vs. 31.98) and lamellae under fourth fingers (means = 13.51, vs. 12.71) and toes (means = 17.03, vs. 16.24) (Table 3).

Differences in measurements of *T. nattereri* compared with *T. yomtovi* sp. n. result in distinct body proportions: axilla–groin length/snout–vent length (means = 0.44, vs. 0.46); head length/snout–vent length (means = 0.27, vs. 0.28); lower arm length/snout–vent length (means = 0.18, vs. 0.16); and shank length/snout–vent length (means = 0.21, vs. 0.19) (Table 3).

#### *Description of neotype*

Body cylindrical, long and relatively wide head and body, long and narrow neck with two well-developed calcium sacs, long snout, long and well-developed limbs and tail broken (Figure S5).

Rostral large, convex, polygonal, partially divided by a median cleft and in broad contact with internasals, upper nasal and first infralabial. Viewed dorsally, rostral is about two times wider than long and posteriorly reaching beyond nostril by about a third of its length. A pair of large internasal scales, irregularly rectangular, in long, medial contact with each other medially, forming a long suture with median cleft of rostral, bordered lateroposteriorly by one loreal scale on each side and posteriorly by two postinternasal scales. Postinternasal scales irregularly pentagonal, similar in size to internasal scales. Frontal scales polygonal, smooth and subimbricate, differing in size. Supraocular scales irregularly hexagonal, smooth and subimbricate, with rounded lateromedial margins. Interorbital scales polygonal, longer than wide, similar in size or slightly smaller than adjacent supraoculars. Seventeen transverse scales across the medial interorbital region. Palpebral fold with smooth scales, varying from subimbricate to feebly granular. Supraciliary scales smooth, varying from imbricate to subimbricate. Parietal and occipital scales polygonal (most of them irregularly hexagonal), smooth, feebly granular and subimbricate, differing in size. Scales on dorsal surface of neck smooth, feebly granular, becoming gradually imbricate towards dorsal surface of body.

Nostril directed lateroposteriorly, bordered by four scales: rostral anteriorly and ventrally, upper nasal dorsally, lower nasal posteriorly and first infralabial ventrally and posteriorly. Two slightly longer than wide nasal scales; lower ones slightly larger than upper nasals and about half the size of internasals. Loreal scales similar in shape and size to frontal scales. Eye large, pupil vertical. Temporal scales feebly granular, subimbricate. Large, round ear opening. Scales on lateral surface of neck varying between granular and feebly granular, subimbricate, in oblique and longitudinal rows. Supralabials 10–11.

Mental large, convex, as long as wide and similar in width to rostral, forming an acute angle posteriorly, reaching level of the suture between first and second

infralabials. Two pairs of large postmentals. Scales of first pair trapezoidal, wider than long, in broad, anterior contact with mental, laterally with the first infralabial and medially with each other. Scales of second pair of postmentals irregular trapezoidal with rounded posterior margins, similar in size among them, and slightly smaller than scales of first pair. Scales of second pair in contact with first and second infralabials and separated from each other by two gular scales. Submandibulars in distinct rows of 6–8 scales (one row on each side); first 3–4 submandibulars larger than posterior ones. Gular scales polygonal to roundish, smooth, feebly granular, subimbricate, nearly subequal, gradually becoming obtuse, then smooth, imbricate, wider than long posteriorly to level of end of mandible, becoming gradually larger and finally about as wide as long towards forelimb insertion. Thirty-two gular scales. Infralabials 9–10, first three rectangle-shaped and taller than long, fourth trapezoidal, taller than long, and similar in size to third, fifth to ninth or tenth with rounded or irregular margins ventrally, decreasing gradually in size posteriorly.

Dorsal scales smooth, imbricate, in oblique and longitudinal rows, 56 middorsal scales from anterior margin of forelimbs to posterior margin of hind limbs. Flank scales similar in shape to, but slightly smaller than dorsolateral scales, 53 scales around midbody. Ventral scales smooth, imbricate, slightly larger than scales on flanks, in oblique and longitudinal rows, 51 midventral scales from anterior margin of forelimbs to preanal plate. Preanal pores absent. Tail broken. Two well-developed postanal sacs on ventral surface of base of tail, and two acute, pointed, granular scales directed posterodorsally on ventrolateral surfaces on each side. Scales on dorsal surface of limbs smooth, imbricate, varying from similar in size to slightly larger than scales on dorsal surface of body. Scales on ventral surface of forelimbs pointed, varying from subimbricate to obtuse, smaller than scales on dorsal surface of forelimbs. Scales on ventral surface of upper hind limbs similar in shape and size to those on dorsal surface of hind limbs, and on ventral surface of lower hind limbs similar to scales on ventral surface of forelimbs, smaller than those on dorsal surface of hind limbs. Posterior surface of thighs with obtuse to roundish, small scales. Ventral aspect of fingers and toes with single and uncarinate subdigital lamellae, 14 lamellae under fourth fingers and 18 lamellae under fourth toes. Claws long and distinct.

#### *Measurements of neotype (in millimetres)*

Snout–vent length = 28.6; axilla–groin length = 13.0; head depth = 3.1; head width = 4.5; head length = 7.8; neck length = 5.6; lower arm length = 4.9; shank length = 5.9; tail broken; mass (taken shortly after collection): 0.8 g.

*Colouration in preservative (based on neotype)*

Dorsal surface of head cream, with several small, brown dots. Dorsal surface of neck cream, with small, sparse brown dots; on the posterior surface of neck, a wide and distinct transverse cream band bordered anteriorly and laterally by brown bands. A wide brown band from rostral and nasal, along loreal region, passing through eye, temporal region, lateral surface of neck, shoulder, to anterolateral surface of body. Dorsal surface of body cream, with two M-shaped cream bands, bordered anteriorly by brown bands; large cream dots irregularly distributed between bands, and anterior to hindlimb insertion. Tail broken: dorsal surface of base of tail cream, with two M-shaped cream bands, bordered anteriorly by brown bands; the first band on the posterior surface of the hindlimb insertion. Dorsal surface of forelimbs, hind limbs, hands and feet with cream dots, and brown between them (lighter on forelimbs, and darker on hind limbs). Flanks cream, with small, sparse brown dots on lower flank surface. Ventral surface of head, neck, body, tail and limbs cream, with few, small, sparsely distributed brown dots.

*Variation*

Table 3 presents a summary of the variation in meristic characters and measurements. Colour pattern presents wide variation among specimens, and variation can be observed in preservative and in life. While specimens collected in Sinai (Egypt) along the coast present similar colour pattern to the neotype (Figure S6A), adult specimens collected in Israel have darker head surfaces; a transverse and narrow cream band on the posterior dorsal surface of neck; dorsal surface of body with several cream dots (varying from large to small ones), bordered or not by brown; and small cream dots on the dorsal surface of limbs (Figure S6B). Juvenile specimens collected in Israel have similar colour patterns as the adults, but with lighter head and body surfaces (Figure S6C).

*Distribution and habitat*

*Tropicolotes nattereri* is distributed along the south and east coast of Sinai, Egypt (on west coast of the Gulf of Aqaba), in Tiran and Sanafir Islands (Saudi Arabia, formerly Egypt), in southern Israel (southern Arava valley as far north as Yotvata and Eilat mountains) and in south-western Jordan (Figure 3).

*Tropicolotes nattereri* is a small, nocturnal and terrestrial species. It inhabits rocky areas and desert flatlands but is absent from sands (personal observations). Baha El Din (1994) claimed it regularly climbs low rocks and vegetation. Our own observations are mostly of terrestrial activity, sometimes very low on acacia trunks (genus *Vachellia*). Field guides and books about the

reptile fauna of Israel presenting the distribution of *T. nattereri* species group (Arbel, 1984; Bar & Haimovitch, 2012, 2018; Bar et al., 2021; Bouskila & Amitai, 2001) use natural history data that refer to *T. yomtovi* sp. n. rather than *T. nattereri* sensu stricto. Although, data in Werner (2016) probably refer to both *T. nattereri* and *T. yomtovi* sp. n.

*Remarks*

Descriptions of new species of *Tropicolotes* have often mentioned *T. nattereri* as diagnosed by having smooth lamellae under fingers and toes (Krause et al., 2013; Machado et al., 2019; Rajabizadeh et al., 2018; Wilms et al., 2010). However, this species, and its sister taxon (*T. yomtovi* sp. n., Figure 4), does not have smooth lamellae, but uncarinate lamellae under fingers and toes, as presented by Baha El Din (1994) and Shifman et al. (1999).

*Tropicolotes yomtovi* sp. n.

(Figures 1–4, Tables 1–3; Figures S1–S5, S8–S9, and Table S1).

urn:lsid:zoobank.org:act:587DE30E-D73F-4EBA-97D1-534B006A8A1D.

*Tropicolotes nattereri* Loveridge (1947, in part); Baha El Din (1994, in part); Shacham and Shifman (1998); Shifman et al. (1999, in part, Figure 2C–D); Bouskila and Amitai (2001, in part); Disi et al. (2001); Modrý et al. (2004); Sindaco and Jeremcenko (2008, in part); Al-Quran (2009); Wilms et al. (2010, in part); Disi (2011); Bar and Haimovitch (2012, in part); Krause et al. (2013, in part); Disi et al. (2014); Sindaco et al. (2014); Handal et al. (2016); Werner (2016, in part); Bar and Haimovitch (2018, in part); Machado et al. (2019, in part); Meiri et al. (2019, in part); Pola et al. (2020); Bar et al. (2021, in part).

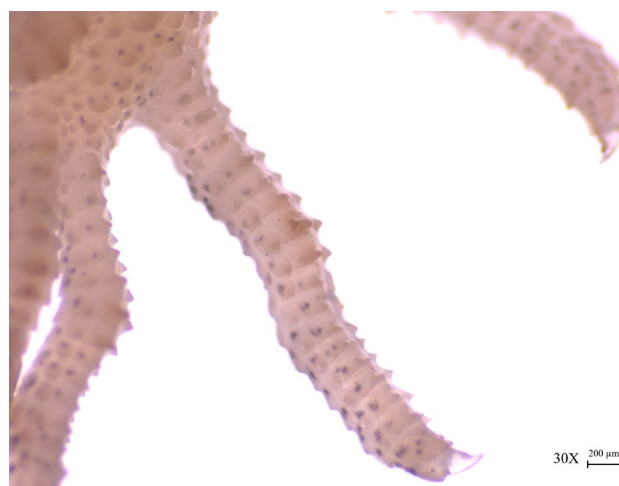


FIGURE 4 Uncarinate subdigital lamellae (holotype of *T. yomtovi* sp. n., TAU.R 19032)

*Tropicolotes nattereri* "A" Machado et al. (2021).

*Tropicolotes steudneri* Haas (1943); Haas (1951); Pasteur (1960); Minton et al. (1970, in part); Arbel (1984, in part); Werner (1988, in part); Kluge (1993, in part); Disi (1996).

*Tropicolotes steudneri nattereri* Hoofien (1972).

#### Holotype

TAU.R 19032, adult, female\*, collected (under permit 42124/2018 from the Israel Nature and Parks Authority) on 27 March 2019 by Shai Meiri, at Holland Park, Eilat, Israel (29.57° N, 34.96° E) (Figure S8).

#### Paratypes

TAU.R 19033, male\*, same collection details and permit as the holotype; BEV 10886, male\*, collected on 28 March 2010 by P. Geniez and G. Geniez, at 'Piste du Bait Ali Camp', W of Wadi Rum, Jordan (29.69° N, 35.43° E); CAS 148526–27, males\*, collected on 15 June 1978 by J. Gasperetti, at Haql, Saudi Arabia (29.30° N, 34.95° E); BMNH1978.368, male\*, collected on 15 June 1978 by J. Gasperetti, at Haql, Saudi Arabia (29.30° N, 34.95° E); NMP6V 71082, collected in 1998, at Aqaba, Jordan (29.56° N, 35.03° E).

#### Referred specimens

A list of specimens in Table S1.

#### Diagnosis

*Tropicolotes yomtovi* sp. n. is distinguished from all other species of *Tropicolotes* by the combination of the following characters: (1) unicarinate lamellae under fingers and toes; (2) mean snout–vent length = 22.24 mm; (3) mean axilla–groin length = 10.20 mm; (4) mean head length = 6.17 mm; (5) mean lower arm length = 3.56 mm; (6) mean shank length = 4.24 mm; (7) mean number of interorbital scales = 15.31; (8) mean number of supralabials = 9.05; (9) mean number of infralabials = 7.69; (10) mean number of gular scales = 31.98; (11) mean number of lamellae under fourth fingers = 12.71; and (12) mean number of lamellae under fourth toes = 16.24.

#### Comparison with other species

*Tropicolotes yomtovi* sp. n. differs from all other species of *Tropicolotes* (*T. algericus*, *T. bisharicus*, *T. chirioi*, *T. confusus*, *T. hormozganensis*, *T. naybandensis*, *T. nubicus*, *T. scortecii*, *T. somalicus*, *T. steudneri*, *T. tassiliensis*, *T. tripolitanus apoklomag*, *T. tripolitanus occidentalis*, *T. tripolitanus tripolitanus* and *T. wolfgangboehmei*), except *T. nattereri*, in having unicarinate lamellae under fourth fingers and toes (vs. tricarinate lamellae). It differs from *T. nattereri* in having shorter snout–vent (means = 22.24 mm, vs. 23.57 mm), head (means = 6.17 mm, vs. 6.63 mm),

axilla–groin (means = 10.20 mm, vs. 10.45 mm), lower arms (means = 3.56 mm, vs. 4.21 mm) and shanks (means = 4.24 mm, vs. 5.00 mm); fewer number of supralabials (means = 9.05, vs. 9.62), infralabials (means = 7.69, vs. 8.05), gulars (means = 31.98, vs. 33.51) and lamellae under fourth fingers (means = 12.71, vs. 13.51) and toes (means = 16.24, vs. 17.03) (Table 3). Differences in measurements with *T. nattereri* result in distinct body proportions: axilla–groin length/snout–vent length (means = 0.46, vs. 0.44), head length/snout–vent length (means = 0.28, vs. 0.27), lower arm length/snout–vent length (means = 0.16, vs. 0.18) and shank length/snout–vent length (means = 0.19, vs. 0.21) (Table 3).

#### Description of holotype

Body cylindrical, long and wide head and body, relatively short and wide neck, short snout, relatively short limbs and long tail (1.1 times the snout–vent length) (Figure S7).

Rostral large, convex, polygonal, partially divided by a median cleft and in broad contact with internasals, upper nasal and first infralabial (on the left side, it also contacts a small loreal scale). Viewed dorsally, rostral is about twice as wide as long, and posteriorly reaching beyond nostril by about a half of its length. A pair of small and narrow inter-nasal scales, irregularly pentagonal, in short, medial contact with each other medially, not forming a long suture with median cleft of rostral, bordered lateroposteriorly by one loreal scale on the right side and two on the left, and posteriorly by two postinternasal scales. Postinternasal scales irregularly hexagonal, similar in size to, or slightly larger than internasal scales. Frontal scales polygonal, subimbricate, varying from smooth to feebly granular, differing in size. Supraocular scales hexagonal, subimbricate and feebly granular. Interorbital scales polygonal (most of them hexagonal), longer than wide and larger than adjacent supraoculars. Sixteen transverse scales across the medial interorbital region. Palpebral fold with scales varying from smooth, subimbricate to feebly granular. Supraciliary scales varying from smooth, imbricate to feebly granular and subimbricate. Parietal and occipital scales polygonal (most of them irregularly hexagonal), feebly granular and subimbricate, differing in size. Scales on dorsal surface of neck feebly granular, becoming gradually imbricate towards dorsal surface of body.

Nostril directed lateroposteriorly, bordered by four scales: rostral anteriorly and ventrally, upper nasal dorsally, lower nasal posteriorly, and first infralabial ventrally and posteriorly. Two slightly longer than wide nasal scales, similar in size and shape among them; upper one on the right side larger than internasal; and upper one on the left side smaller than internasal. Loreal scales similar in shape and size to frontal scales. Eye large, pupil vertical. Temporal scales feebly granular, subimbricate. Small, oval

ear opening. Scales on lateral surface of neck varying from granular and subimbricate to feebly granular and imbricate, in oblique and longitudinal rows. Supralabials 9–10.

Mental large, convex, as long as wide and similar in width to rostral, forming a triangular angle posteriorly, reaching level of the suture between first and second infralabials. Two pairs of large postmentals. Scales of first pair pentagonal, wider than long, in broad, anterior contact with mental, laterally with the first infralabial (touching second supralabial) and medially with each other. Scales of second pair of postmentals polygonal with irregular posterior margins, similar in size among them, and smaller than scales of first pair; scales of second pair in contact with second infralabial and separated from each other by two gular scales. Submandibulars in distinct rows of five scales (one row on each side); first 1–2 submandibulars larger than posterior ones. Gular scales hexagonal to roundish, smooth, feebly granular, subimbricate, differing in size (anterior and lateral ones larger than medial ones), gradually becoming obtuse, then smooth, imbricate, wider than long posteriorly to level of end of mandible, becoming gradually larger and finally about as wide as long towards forelimb insertion. Thirty-two gular scales. Eight infralabials, first four rectangle-shaped varying from longer than tall to taller than long, fifth trapezoidal, longer than tall and slightly larger than fourth, fifth to eighth with rounded or irregular margins ventrally, decreasing gradually in size.

Dorsal scales smooth, imbricate, in oblique and longitudinal rows, 55 middorsal scales from anterior margin of forelimbs to posterior margin of hind limbs. Flank scales similar in shape and size to dorsolateral scales, 55 scales around midbody. Ventral scales smooth, imbricate, similar in size to scales on flanks, in oblique and longitudinal rows, 49 midventral scales from anterior margin of forelimbs to preanal plate. Two inconspicuous preanal pores bordering anteriorly preanal plate, one pore per scale, separated by one scale. Tail complete and intact, with smooth, imbricate scales on dorsal, lateral and ventral surfaces, similar in size to or slightly larger than scales on dorsal surface of body. Two inconspicuous postanal sacs on ventral surface of base of tail, and two granular, imbricate scales directed posterodorsally on ventrolateral surfaces of base of tail on each side. Scales on dorsal surface of limbs smooth, imbricate, varying from similar in size to slightly larger than scales on dorsal surface of body. Scales on ventral surface of forelimbs pointed, varying from subimbricate to obtuse, smaller than scales on dorsal surface of forelimbs. Scales on ventral surface of upper hind limbs similar in shape and size to those on dorsal surface of hind limbs and on ventral surface of lower hind limbs similar to scales on ventral surface of forelimbs, smaller than those on dorsal surface of hind limbs. Posterior surface of

thighs with obtuse to roundish, small scales. Ventral aspect of fingers and toes with single and uncarinate subdigital lamellae, 13–14 lamellae under fourth fingers and 18 lamellae under fourth toes. Claws long and distinct.

#### *Measurements of holotype (in millimetres)*

Snout–vent length = 25.4; axilla–groin length = 11.9; head depth = 2.9; head width = 5.1; head length = 7.0; neck length = 4.0; lower arm length = 4.6; shank length = 5.2; tail length = 28.3 (1.1 times snout-vent length); mass = 0.4 g (measured in life).

#### *Colouration in preservative (based on holotype)*

Dorsal surface of head cream, with several small, brown dots. Dorsal surface of neck cream, with small, sparse brown dots; on the transition between the posterior surface of neck and anterior surface of body (between forelimbs insertion), a wide and distinct transverse cream band bordered anteriorly by a brown band. A wide brown band from rostral and nasals, along loreal region, passing through eye, to temporal region; on the anterolateral surface of neck the band is absent, but it appears again on the posterior surface of neck; absent on shoulders and flanks. Dorsal surface of body cream, with two M-shaped cream bands, bordered anteriorly by brown bands; a few, sparse cream dots irregularly distributed between bands, and anterior to hindlimb insertion; a third M-shaped cream band bordered anteriorly by a brown band between the hindlimb insertion. Tail cream with twelve transverse, cream bands bordered anteriorly by brown bands; bands become inconspicuous from the anterior surface of tail to the posterior surface (almost indistinct near the tip of the tail). Dorsal surface of forelimbs, hind limbs, hands and feet cream, with several sparse, small brown dots; on thighs, the small brown dots form inconspicuous and relatively large brown dots; on the dorsal surface of lower hind limbs, dots are organized in 2–3 oblique bands. Flanks cream, with small, sparse brown dots on upper flank surface and relatively large ones on lower surface of it. Lateral surface of tail cream, with several sparse, small brown dots. Ventral surface of head, neck, body, tail and limbs cream, with few, small, sparsely distributed brown dots.

#### *Variation*

Table 3 presents a summary of the variation in meristic characters and measurements. Specimens present extremely variable colouration patterns along the distribution of the species, and variations can be observed in preservative and in life. Other specimens observed in the type locality of *Tropiocolotes yomtovi* sp. n. have similar patterns to the holotype (Figure S8A), as do specimens collected in Jordan (Figure S8B) and Saudi Arabia have.



Specimens from the Negev Desert do not present dorsal bands but have small white dots (Figure S8D). Specimens from near the Dead Sea and in the northern Arava Valley show a pattern varying from presenting large cream or white dots bordered by transverse brown bands, to having cream or white transverse bands also bordered anteriorly by brown (Figure S8E), sometimes having darker surfaces of the head and body then specimens from other regions (Figure S8C).

#### Etymology

The specific epithet is a noun in the genitive case honouring Yoram Yom-Tov (born 1938), the former curator of terrestrial vertebrates at the Tel Aviv University Zoological Museum (now the Steinhardt Museum of Natural History, Tel Aviv University), a superb zoologist, teacher, mentor and colleague, who introduced some of us to these marvellous tiny geckos.

#### Distribution and habitat

*Tropicolotes yomtovi* sp. n. as currently understood is distributed from the Judean Desert (Israel and the Palestinian Authority) in the north, along the west bank of the Dead Sea (Israel and the Palestinian Authority), along the Negev Desert (Israel) and adjacent areas in north Sinai (Egypt), the Arava Valley (Israel and Jordan), Wadi Rumm (south-west Jordan), to the coastal area of the Red Sea in Israel, Jordan and Saudi Arabia (north and west coast of the Gulf of Aqaba) (Figure 3). In southern Israel, it is in partial sympatry with *T. nattereri*, at the southern part of its range. Pola et al. (2020) reported it from the east bank of the Dead Sea, in Jordan. The northernmost distribution record of *T. yomtovi* sp. n. was presented in Shacham et al. (2016) as 31.85N. In Israel, we have observed this species ranging from 360 m below sea level (Old Ein Gedi, 31.46N, 35.39E) to 600 m above sea level (Lipa Gal Observatory, 30.82N, 34.84E).

Haas (1943) found specimens under single large stones or among rubble on the hill sides, which agrees with our own observations. According to Shifman et al. (1999), it inhabits mainly the rocky desert but has been found also in sandy areas. The same authors found it active only at night and once climbing a concrete wall. We have observed them active only at night, invariably on the ground and never on sand. We assume individuals were actively foraging. They can be locally abundant, hiding under rocks by day. Females lay a single egg. The diet is composed of tiny arthropods. All natural history data reported in field guides and herpetology books about the reptile fauna of Israel referring to *Tropicolotes steudneri* or *T. nattereri* (e.g. Arbel, 1984; Bar & Haimovitch, 2012, 2018; Bar et al., 2021; Bouskila & Amitai, 2001) should be referred to this species (Werner, 2016, probably refers both to *T. yomtovi*

sp. n. and *T. nattereri*). The body temperature of one active individual measured by SM was 26°C. Body temperatures of 12 inactive animals found under rocks by day or evening ranged between 23.2 and 35.4°C (mean = 32.3°C), at air temperatures between 19.5 and 35.6°C (mean = 30.7°C).

## 4 | DISCUSSION

This study provides the largest sampling to date and the first molecular assessment of the intraspecific diversity within the *Tropicolotes nattereri* species complex. The inferred topologies in our phylogenetic reconstructions are consistent with previous studies on *Tropicolotes* regarding the phylogenetic position of *Tropicolotes nattereri* within the genus (Machado et al., 2021; Metallinou et al., 2012). The molecular results of the *T. nattereri* species complex were congruent across analyses and genes and generally support a deep segregation of two main groups: *T. nattereri* and *T. yomtovi* sp. n. This result has first been reported by Machado et al. (2021). The absence of allele sharing in the nuclear gene fragments where the two groups co-occur (Figure 2) suggests restricted gene flow and reproductive isolation and hence that the two clades A and B–D constitute valid species. *Tropicolotes yomtovi* sp. n. contains three partially sympatric subclades (B–D): the genetic distances at the mitochondrial level among them (2–4% in *12S* and 6–7% in *ND2*) are lower than the interspecific distances among the other species of the genus, and they exhibit extensive allele sharing at the two nuclear markers analyzed. We thus treat them as conspecific.

The taxonomy of the *Tropicolotes nattereri* species group (including *T. nattereri* and *T. yomtovi* sp. n.) has always been permeated by instabilities. *Tropicolotes nattereri* was described using two syntypes from different sides of the Gulf of Aqaba (Figure 3). Later, it was synonymized with *T. steudneri*, and incorrect diagnostic characters (e.g. tricarinate subdigital lamellae) have been mentioned in the literature after its revalidation. Therefore, this species group has been one of the most taxonomically problematic in this genus. *Tropicolotes nattereri* has been supported as a distinct species based on characters such as having larger eyes, and longer, more slender limbs than its supposed closest related species, *T. steudneri* (Leviton & Anderson, 1972; Loveridge, 1947; Steindachner, 1901). Flowers (1933) was the first to doubt its validity. He was followed by Haas (1951) and Loveridge (1947). Despite presenting it in a list of valid species, Loveridge (1947: 51) wrote that ‘this alleged species is doubtfully distinct from *steudneri*’, concluding that records from western Arabia and Sinai actually belong to *T. steudneri*. Pasteur (1960)

was the first to compare species presumably belonging to *T. steudneri* and *T. nattereri* to confirm the validity of *T. nattereri*. However, he used a specimen from Israel as voucher of *T. steudneri* and another from Libya as *T. nattereri* for comparisons. Neither species inhabits the regions Pasteur (1960) mentioned. Guibé (1966) was not convinced by Pasteur's findings and concluded that the Libyan specimen of *T. nattereri* was actually a variation of *T. steudneri*. He was followed by Minton et al. (1970), who considered specimens from Israel as variation of *T. steudneri*. Hoofien (1972) considered *T. nattereri* as a subspecies, *T. steudneri nattereri*. Arnold (1977), Kluge (1993) and Anderson (1999), formally recognized *T. nattereri* as a junior synonym of *T. steudneri*.

The major contribution to the taxonomy of *Tropicolotes nattereri*, with respect to its distinctiveness, was produced by Baha El Din (1994). Analyzing specimens collected in northern Arabia, Israel and Sinai, and comparing them to specimens collected in the African part of Egypt (west of the Suez Canal), Baha El Din (1994) confirmed the original characters presented by Steindachner (1901) (large eyes, slender and long limbs) as diagnostic. He included uncarinate lamellae under fingers and toes as further and easier way to distinguish *T. nattereri* from *T. steudneri* (the latter having tricarinate lamellae under fingers and toes). The author also included the presence of 4–5 dark dorsal bands as a character not found in *T. steudneri*. Baha El Din (1994) was the first to correctly draw the whole distribution of *T. nattereri*, in Sinai, Israel, Jordan and Saudi Arabia, excluding it from Africa. Based on the findings of Baha El Din (1994), Shifman et al. (1999) increased the morphological sampling and improved the morphological character selection and analytical methods. In addition to the diagnostic characters presented by Baha El Din (1994), Shifman et al. (1999) suggested that the lateral scales on the fourth toes in *T. steudneri* are more spinous than in *T. nattereri*. Even though presenting comprehensive analyses of the differences between *T. steudneri* and *T. nattereri*, the works of neither Baha El Din (1994), nor Shifman et al. (1999), have been considered by subsequent studies that compare diagnostic features of *Tropicolotes* species. Krause et al. (2013), Machado et al. (2019), and Wilms et al. (2010) diagnosed *T. nattereri* as having smooth subdigital lamellae, although it has uncarinate lamellae (Figure 4, see also Figure 1 in Shifman et al., 1999). Smooth subdigital lamellae are not observed in *T. yomtovi* sp. n., *T. nattereri* or any other *Tropicolotes* species. Ribeiro-Júnior et al. (2022) redefined *T. steudneri* and assigned a neotype. Together with the results presented herein, we define the characters: (1) subdigital lamellae, and (2) number of dorsal scales, as the ones that easily distinguish the *T. nattereri* species group from *T. steudneri* (uncarinate lamellae [Figure 4], and 42–59 dorsals in *T. nattereri* and

48–60 in *T. yomtovi* sp. n.; vs. tricarinate lamellae, and 61–66 dorsals in *T. steudneri*).

In the original description of *Tropicolotes nattereri*, Steindachner (1901) did not designate museum numbers for the syntypes nor mention a collection where they were catalogued. None of the authors who studied the taxonomy of *Tropicolotes* species, after *T. nattereri* was described, mentions examining these specimens. Bauer and Günther (1991) provided a list of type specimens housed in the Zoological Museum (Museum für Naturkunde), Berlin (ZMB), where it could have been catalogued, but the syntypes were not among the specimens nor in the list of lost/destroyed material. We (M. A. Ribeiro-Júnior, and P. Wagner) searched for these animals in many European collections, including the Naturhistorisches Museum Wien, where Steindachner worked, but we did not find them. Uetz et al. (2020) considered the types lost. We suggest that (1) taxonomic entities need to be strictly defined; (2) descriptions of characters and states of characters need to be precise, forming diagnostic characters for those entities; (3) the taxonomic status of *T. nattereri* has been repeatedly questioned (Anderson, 1999; Arnold, 1977; Flowers, 1933; Guibé, 1966; Haas, 1951; Kluge, 1993; Loveridge, 1947; Minton et al., 1970), primarily because of its vague relationship with *T. steudneri*; (4) *T. nattereri* has had diagnostic characters incorrectly assigned for it (Krause et al., 2013; Machado et al., 2019; Wilms et al., 2010); (5) *T. nattereri* was originally described from a type series we consider to have comprised of two different species; (6) its original type specimens are lost; (7) the morphological data available in the original description are limited, and to a certain degree generic; and (8) the diversity in the genus *Tropicolotes* is still far from being known and described (Machado et al., 2021), with diagnostic characters in need to be redefined, and for that type series need to be (re)analyzed (Ribeiro-Júnior et al., 2022). Designating a neotype for *T. nattereri* is therefore called for.

Steindachner (1901) used two syntypes to describe *Tropicolotes nattereri*, one from Saudi Arabia and another from Sinai (Egypt). These localities are on opposite sides of the Gulf of Aqaba and are inhabited by different species (species of the clade A in the Sinai and species of the clades B–D in Saudi Arabia). In order to allocate the nomen *Tropicolotes nattereri* to one of these two species, we designated as neotype of *T. nattereri* a specimen from the Sinai belonging to the clade A. In theory, a lectotype designation could be sufficient, but considering that we have only genotyped a small number of specimens, that morphological identification of these two species remains difficult and that the number of specimens examined is still low, we cannot be sure that only one species occurs in

the Sinai Peninsula or in northwestern Saudi Arabia and we cannot be sure of the identification of the specimen illustrated in Steindachner (1901). A mere lectotype designation would thus maintain the risk of nomenclatural instability if the two species were later discovered to be sympatric in part of the original type locality. We thus designate a neotype of *Tropicolotes nattereri* among one of the specimens that we have genotyped to ensure a permanent allocation of this nomen to one of the two species we recognized in this work.

The Saudi Arabian animals are morphologically similar to those from further north in Israel, which we here described as *T. yomtovi* sp. n. Due to the absence of specimens collected in Nuweiba (Sinai, Egypt), the original type locality of *T. nattereri*, we choose a voucher from the closest locality sampled (Dahab, about 70 km south of Nuweiba).

Meristic data of the *Tropicolotes nattereri* group are scarce in the literature. Minton et al. (1970) and Pasteur (1960) presented data for *T. yomtovi* sp. n. (as *T. steudneri*). All ranges in Pasteur (1960) match with variation we observed (in parentheses): midbody scales 48–49 (42–55); lamellae under the fourth toes 15–16 (13–20); and supralabials 7–9 (7–11). Between Minton et al. (1970) and our data (in parentheses), we can observe similarities in supralabials 7–8 (7–11) and lamellae under the fourth toe 14–16 (13–20), but Minton et al. (1970) found 5–7 infralabials (7–9), and he reported 41–48 dorsal scales (48–60 in our sample). These differences can be a result of varying definitions of the characters, affecting total counts or even mistakes in counting. Minton et al. (1970) also report Israeli specimens as having tricarinate subdigital lamellae, a character state not found in either species of the *T. nattereri* group. Qualitative characters (contact between postmentals and infralabials; medial contact between postmentals; size of internasals), and colour patterns (presence of dorsal bands and the number of them; number of bands on tail), described in Minton et al. (1970) and Pasteur (1960), are extremely variable in *T. yomtovi* sp. n.. Therefore, we do not consider them as diagnostic. Baha El Din (1999) mentioned that *T. nattereri* (the author does not offer a list of specimens allowing for the allocation of specimens to clades within the species group; hence, we assume that his data apply to *T. nattereri* and *T. yomtovi* sp. n.) has fewer than 50 dorsal scales, but variation in this group is 42–60 based on our data.

Shifman et al. (1999) presented the best and most detailed morphological information about the *Tropicolotes nattereri* group. Despite not recognizing two species, the authors found that limb lengths, and the number of supralabials and infralabials were negatively correlated with latitude. Similar results were found by us, considering that *T. yomtovi* sp. n. is distributed in the northern portion

and *T. nattereri* in the south of the group's geographical range. *Tropicolotes yomtovi* sp. n. has shorter limbs and fewer labials. Two meristic characters are comparable between our study and Shifman et al. (1999): the numbers of dorsal scales and supralabials. Numbers of supralabials are similar (8–11 in Shifman et al., 1999, and 7–11 in our study), but Shifman et al. (1999) reported 38–46 dorsals, vs. 42–60 found in our study. Other differences presented in Shifman et al. (1999) could not be compared with our data because they are associated with sexual dimorphism. Shifman et al. (1999) sexed specimens 'by appearance and hemipenial swelling', but appearance is a vague criterion and hemipenial swelling varies between reproductive and nonreproductive seasons and ontogenetic stages. Other characteristics often used to determine sex in *Tropicolotes*, such as the presence of well-developed calcium sacs or pores, also vary among specimens of the same sex. Colour pattern was discussed in Shifman et al. (1999), who wrote individuals have 4–5 blackish transverse lines, bordered posteriorly by a white margin. They mentioned that 'this pattern may be faint, partial or obscured by additional markings'. Bands on the dorsal surface of the body can be found in *T. nattereri* and *T. yomtovi* sp. n., but in some specimens, only dots are found (white or brown; Figure S9). This is not because the bands are faint, partial or obscured: sometimes they are simply absent. Our results indicate that both species of the *T. nattereri* group are highly polymorphic in their colour pattern.

Phylogenetic studies addressing the species-level relationships in *Tropicolotes* are scarce and recent. There are four studies. Bauer et al. (2013) produced the first molecular phylogeny for the Palearctic naked-toed geckos, including four species of *Tropicolotes* (*T. nubicus*, *T. somalicus*, *T. steudneri* and *T. tripolitanus*). The genus was not monophyletic in their analyses, with *T. tripolitanus* (the type species of the genus) retrieved as sister to *Stenodactylus*, rather than to other *Tropicolotes*, although this pattern was weakly supported. *Tropicolotes nattereri* was not included in their analyses. Krause et al. (2013) presented the first morphological phylogenetic hypothesis for the genus, including all described species of *Tropicolotes* by that time. *Tropicolotes nattereri* was recovered as part of the group composed of *T. bisharicus*, *T. naybandensis*, *T. nubicus*, *T. scoreccii*, *T. steudneri* and *T. wolfgangboehmei*, named by the authors as *T. steudneri/nattereri* clade. A second group, containing *T. algericus*, *T. somalicus*, *T. tripolitanus tripolitanus* and *T. t. occidentalis*, was presented as sister clade to *T. steudneri/nattereri*. Based on molecular data, Machado et al. (2019) recovered a topology generally similar to the one presented in Krause et al. (2013), but with *T. somalicus* included in the group containing *T. steudneri/nattereri*, rather than in the *T. tripolitanus* group. Within the *T. steudneri/nattereri* group, they found

that *T. nattereri* was the first species to diverge. Increasing their molecular sampling, Machado et al.'s (2021) results were similar to Machado et al. (2019), but they recovered two deep lineages within *T. nattereri* nearly sympatric in southern Israel and Jordan. The lineage they named as *T. nattereri* B is our *T. nattereri* sensu stricto, and the lineage they referred to as '*T. nattereri* A' is the new species described herein, *T. yomtovi* sp. n.

The genetic similarity between the subclades in *Tropicolotes yomtovi* sp. n. implies a relatively recent divergence and shared ancestral evolutionary history. According to Machado et al. (2021), the split between *T. nattereri* and *T. yomtovi* sp. n. probably occurred around 8 Mya due to habitat fragmentation resulting from the complex topographic profile and climatic conditions that prevailed in the southern Levant. Based on the position of *T. nattereri* in our mitochondrial phylogeny, it may be cautiously assumed that because *T. nattereri* was the first to diverge, the group originated in the south of the distribution of the species group. However, we highlight that biogeographical studies are still needed to elucidate the evolution and distribution of this group in the Middle East, as well as distributional shifts that may have occurred during the Pleistocene ice ages. Although targeted by phylogenetic studies during the last decade (Bauer et al., 2013; Krause et al., 2013; Machado et al., 2019, 2021), the taxonomic status of most of the species in *Tropicolotes* still needs clarification, as we showed here. Machado et al. (2021), and Ribeiro-Júnior et al. (2022), also showed that the cryptic diversity in this genus is still far from being known, with many species awaiting descriptions, and diagnostic characters in need to be redefined.

## ACKNOWLEDGMENTS

We are grateful to the following curators and staff from museums who granted access to specimens: L. Scheinberg and E. Ely (California Academy of Science, San Francisco), J. Streicher (Natural History Museum, London), A. Resetar and J. Mata (Field Museum, Chicago), L. Vonnahme (American Museum of Natural History, New York) and J. Moravec (Národní Muzeum, Prague). We thank Aviad Bar and Jonathan Ben-Simon for sending pictures of specimens in life. This work was supported by the Gans Collections and Charitable Fund Inc. [M.A.R.-J. grant], SYNTHESYS<sup>+</sup>, Synthesis of Systematic Resources funded by the European Commission [M.A.R.-J. grants: ES-TAF-1276; GB-TAF-2393; CZ-TAF-1260; DE-TAF-2418], the Rector scholarship, Tel Aviv University [M.A.R.-J. postdoctoral fellowship] and the Alexander and Eva Lester Fund scholarship, I. Meier Segals Garden for Zoological Research [M.A.R.-J. postdoctoral fellowship]. We thank A. Bauer, and an anonymous reviewer, for comments and suggestions that greatly improved our study.

## CONFLICT OF INTEREST

The authors declare that they have no conflict of interest.

## AUTHOR CONTRIBUTIONS

Shai Meiri contributed to the study conception, and Shai Meiri, Marco Ribeiro-Júnior and Karin Tamar to the study design. Material preparation, data collection and analysis were performed by all authors. The first draft of this manuscript was written by Marco Ribeiro-Júnior and Karin Tamar. All authors commented on previous versions of the manuscript and have revised it.

## ORCID

Marco Antônio Ribeiro-Júnior  <https://orcid.org/0000-0002-0863-6121>

Karin Tamar  <https://orcid.org/0000-0003-2375-4529>

## REFERENCES

- Al-Quran, S. (2009). The herpetofauna of the Southern Jordan. *American-Eurasian Journal of Agricultural and Environmental Sciences*, 6, 385–391.
- Anderson, S. C. (1999). *The lizards of Iran. Contributions to herpetology volume 15*. Society for the Study of Amphibians and Reptiles.
- Arbel, A. (1984). *Zohalim ve-duhayim [Reptiles & amphibians]*. Society for the Protection of Nature & Ministry of Defence Publications.
- Arnold, E. N. (1977). Little known geckos (Reptilia: Gekkonidae) from Arabia with descriptions of two new species from the Sultanate of Oman. *Journal of Oman Studies Special Report*, 1, 81–110.
- Baha El Din, S. M. (1994). A contribution to the herpetology of Sinai. *British Herpetological Society Bulletin*, 48, 18–27.
- Baha El Din, S. M. (1999). A new species of *Tropicolotes* (Reptilia: Gekkonidae) from Egypt. *Zoology in the Middle East*, 19, 17–26. <https://doi.org/10.1080/09397140.1999.10637791>
- Bar, A., & Haimovitch, G. (2012). *A field guide to reptiles and amphibians of Israel*. Privately published.
- Bar, A., & Haimovitch, G. (2018). *A field guide to reptiles and amphibians of Israel*, 2nd ed. The Israeli Nature and Parks Authority Press.
- Bar, A., Haimovitch, G., & Meiri, S. (2021). *Field guide to the amphibians and reptiles of Israel*. Edition Chimaira.
- Bauer, A., & Günther, R. (1991). An annotated type catalogue of the Geckos (Reptilia: Gekkonidae) in the Zoological Museum, Berlin. *Mitteilungen Aus Dem Zoologischen Museum in Berlin*, 67, 279–310. <https://doi.org/10.1002/mmzn.19910670204>
- Bauer, A. M., Masroor, R., Titus-Mcquillan, J., Heinicke, M. P., Daza, J. D., & Jackman, T. R. (2013). A preliminary phylogeny of the Palearctic naked-toed geckos (Reptilia: Squamata: Gekkonidae) with taxonomic implications. *Zootaxa*, 3599, 301–324. <https://doi.org/10.11646/zootaxa.3599.4.1>
- Benjamini, Y., & Hochberg, Y. (1995). Controlling the False Discovery Rate: a practical and powerful approach to multiple testing. *Journal of the Royal Statistical Society: Series B*, 57, 289–300. <https://doi.org/10.1111/j.2517-6161.1995.tb02031.x>
- Bouskila, A., & Amitai, P. (2001). *Handbook of amphibians & reptiles of Israel*. Keter Publishing. [in Hebrew].

- Bruen, T. C., Philippe, H., & Bryant, D. (2006). A simple and robust statistical test for detecting the presence of recombination. *Genetics*, *172*, 2665–2681. <https://doi.org/10.1534/genetics.105.048975>.
- Clement, M., Posada, D., & Crandall, K. A. (2000). TCS: a computer program to estimate gene genealogies. *Molecular Ecology*, *9*, 1657–1659. <https://doi.org/10.1046/j.1365-294x.2000.01020.x>.
- Darriba, D., Taboada, G. L., Doallo, R., & Posada, D. (2012). jModelTest 2: more models, new heuristics and parallel computing. *Nature Methods*, *9*, 772. <https://doi.org/10.1038/nmeth.2109>
- Disi, A. M. (1996). A contribution to the knowledge of the herpetofauna of Jordan. VI. The Jordanian herpetofauna as a zoogeographic indicator. *Herpetozoa*, *9*, 71–81.
- Disi, A. M. (2011). Review of the lizard fauna of Jordan. *Zoology in the Middle East*, *54*, 89–102. <https://doi.org/10.1080/09397140.2011.10648900>
- Disi, A. M., Amr, Z. S., & Hamidan, N. (2014). Diversity, threats, and conservation of the terrestrial and freshwater herpetofauna of Jordan. *Russian Journal of Herpetology*, *21*, 221–233.
- Disi, A. M., Modrý, D., Necas, P., & Rifai, L. (2001). *Amphibians and reptiles of the Hashemite kingdom of Jordan: an atlas and field guide*. Edition Chimaira.
- Flowers, S. S. (1933). Notes on the recent reptiles and amphibians of Egypt, with a list of the species recorded from that kingdom. *Proceedings of the Zoological Society of London*, *1933*, 735–851. <https://doi.org/10.1111/j.1096-3642.1933.tb01617.x>
- Gray, J. E. (1825). A synopsis of the genera of reptiles and amphibia, with a description of some new species. *Annals of Philosophy*, *10*, 193–217.
- Guibé, J. (1966). Contribution a l'étude des genres *Microgecko* Nikolsky et *Tropicolotes* Peters (Lacertilia, Gekkonidae). *Bulletin Du Museum National D'histoire Naturelle*, *38*, 337–346.
- Haas, G. (1943). On a collection of reptiles from Palestine, Transjordan, and Sinai. *Copeia*, *1943*, 10–15. <https://doi.org/10.2307/1437872>
- Haas, G. (1951). On the present state of our knowledge of the herpetofauna of Palestine. *Bulletin of the Research Council of Israel*, *1*, 67–94.
- Hammer, Ø., Harper, D. A. T., & Ryan, P. D. (2001). Past: paleontological statistics software package for education and data analysis. *Palaeontologia Electronica*, *4*, 1–9.
- Handal, E. N., Amr, Z. S., & Qumsiyeh, M. B. (2016). Some records of reptiles from the Palestinian Territories. *Russian Journal of Herpetology*, *23*, 261–270.
- Hoofien, I. H. (1972). *A taxonomic list of the reptiles of Israel and its administered areas according to the status on May 31st, 1972*. Department of Zoology, Tel Aviv University.
- Huson, D. H., & Bryant, D. (2006). Application of phylogenetic networks in evolutionary studies. *Molecular Biology and Evolution*, *23*, 254–267. <https://doi.org/10.1093/molbev/msj030>
- Katoh, K., & Standley, D. M. (2013). MAFFT multiple sequence alignment software version 7: improvements in performance and usability. *Molecular Biology and Evolution*, *30*, 772–780. <https://doi.org/10.1093/molbev/mst010>
- Kearse, M., Moir, R., Wilson, A., Stones-Havas, S., Cheung, M., Sturrock, S., Buxton, S., Cooper, A., Markowitz, S., Duran, C., Thierer, T., Ashton, B., Meintjes, P., & Drummond, A. (2012). Geneious Basic: an integrated and extendable desktop software platform for the organization and analysis of sequence data. *Bioinformatics*, *28*, 1647–1649. <https://doi.org/10.1093/bioinformatics/bts199>
- Kluge, A. G. (1993). *Gekkonoid lizard taxonomy*. International Gecko Society.
- Krause, V., Ahmadzadeh, F., Moazeni, M., Wagner, P., & Wilms, T. (2013). A new species of the genus *Tropicolotes* Peters, 1880 from western Iran (Squamata: Sauria: Gekkonidae). *Zootaxa*, *3716*, 22–38. <https://doi.org/10.11646/zootaxa.3716.1.2>
- Kumar, S., Stecher, G., Li, M., Knyaz, C., & Tamura, K. (2018). MEGA X: Molecular Evolutionary Genetics Analysis across computing platforms. *Molecular Biology and Evolution*, *35*, 1547–1549. <https://doi.org/10.1093/molbev/msy096>
- Leviton, A. E., & Anderson, S. C. (1972). Description of a new species of *Tropicolotes* (Reptilia: Gekkonidae) with a revised key to the genus. *Occasional Papers of the California Academy of Sciences*, *96*, 1–7. <https://doi.org/10.5962/bhl.part.1637>
- Loveridge, A. (1947). Revision of the African lizards of the family Gekkonidae. *Bulletin of the Museum of Comparative Zoology at Harvard*, *98*, 1–469.
- Machado, L., Salvi, D., Harris, D. J., Brito, J. C., Crochet, P. A., Geniez, P., Ahmadzadeh, F., & Carranza, S. (2021). Systematics, biogeography and evolution of the Saharo-Arabian naked-toed geckos genus *Tropicolotes*. *Molecular Phylogenetics and Evolution*, *155*, 106969. <https://doi.org/10.1016/j.ympev.2020.106969>
- Machado, L., Šmíd, J., Mazuch, T., Sindaco, R., Al Shukaili, A. S., & Carranza, S. (2019). Systematics of the Saharo-Arabian clade of the Palearctic naked-toed geckos with the description of a new species of *Tropicolotes* endemic to Oman. *Journal of Zoological Systematics and Evolutionary Research*, *57*, 159–178. <https://doi.org/10.1111/jzs.12226>
- Meiri, S., Belmaker, A., Berkowic, D., Kazes, K., Maza, E., Bar-Oz, G., & Dor, R. (2019). A checklist of Israeli land vertebrates. *Israel Journal of Ecology and Evolution*, *65*, 43–70. <https://doi.org/10.1163/22244662-20191047>
- Metallinou, M., Arnold, E. N., Crochet, P.-A., Geniez, P., Brito, J. C., Lymberakis, P., Baha El Din, S., Sindaco, R., Robinson, M., & Carranza, S. (2012). Conquering the Sahara and Arabian deserts: systematics and biogeography of *Stenodactylus* geckos (Reptilia: Gekkonidae). *BMC Evolutionary Biology*, *12*, 258. <https://doi.org/10.1186/1471-2148-12-258>
- Minton, S. A. Jr, Anderson, S. C., & Anderson, J. A. (1970). Remarks on some geckos from southwest Asia, with descriptions of three new forms and a key to the genus *Tropicolotes*. *Proceedings of the California Academy of Sciences*, *37*, 333–362.
- Modrý, D., Rifai, L., Abu Baker, M., & Amr, Z. (2004). Amphibians and reptiles of the Hashemite Kingdom of Jordan. *Denisia*, *14*, 407–420.
- Múrias dos Santos, A., Cabezas, M. P., Tavares, A. I., Xavier, R., & Branco, M. (2016). tcsBU: a tool to extend TCS network layout and visualization. *Bioinformatics*, *32*, 627–628. <https://doi.org/10.1093/bioinformatics/btv636>
- Oppel, M. (1811). *Die Ordnungen, Familien und Gattungen der Reptilien als Prodrum einer Naturgeschichte derselben*. Joseph Lindauer. <https://doi.org/10.5962/bhl.title.4911>
- Pasteur, G. (1960). Redécouverte et validité probable du Gekkonide *Tropicolotes nattereri* Steindachner. *Comptes Rendus Des Seances Mensuelles, Societe De Sciences Naturelles Et Physique Du Maroc*, *8*, 143–144.

- Peters, W. C. H. (1880). Über die von Hrn. Gerhard Rohlf's und Dr. A. Stecker auf der Reise nach der Oase Kufra gesammelten Amphibien. *Monatsberichte Der Königlich Preussischen Akademie Der Wissenschaften Zu Berlin, 1880*, 305–309.
- Pola, L., Hejduk, V., Winkelhöfer, T., Zika, A., Baker, M. A. A., & Amr, Z. S. (2020). Recent observations on amphibians and reptiles in the Hashemite Kingdom of Jordan. *Jordan Journal of Natural History*, 7, 11–29.
- Rajabizadeh, M., Faizi, H., Anderson, C. S., Zarrintab, M., & Nazarov, R. (2018). Taxonomic status of *Tropicolotes* cf. *steudneri* with a description of a new species of *Tropicolotes* (Reptilia: Squamata: Gekkonidae) in southern Iran. *Zootaxa*, 4388, 283–291. <https://doi.org/10.11646/zootaxa.4388.2.10>
- Rambaut, A., Suchard, M. A., Xie, D., & Drummond, A. J. (2014). *Tracer v1.6*. <http://beast.bio.ed.ac.uk/Tracer>
- Ribeiro-Júnior, M. A. (2018). A new species of *Alopoglossus* lizard (Squamata, Alopoglossidae) from the southern Guiana Shield, northeastern Amazonia, with remarks on diagnostic characters to the genus. *Zootaxa*, 4422, 25–40. <https://doi.org/10.11646/zootaxa.4422.1.2>
- Ribeiro-Júnior, M. A., Koch, C., Flecks, M., Calvo, M., & Meiri, S. (2022). Dwarves in a big world: two new species of *Tropicolotes* (Squamata: Gekkonidae) from the Sahara Desert, with the first detailed skull description to the genus. *Journal of Herpetology*. In press.
- Ronquist, F., Teslenko, M., Van Der Mark, P., Ayres, D. L., Darling, A., Höhna, S., Larget, B., Liu, L., Suchard, M. A., & Huelsenbeck, J. P. (2012). MrBayes 3.2: Efficient Bayesian phylogenetic inference and model choice across a large model space. *Systematic Biology*, 61, 539–542. <https://doi.org/10.1093/sysbio/sys029>
- Rozas, J., Ferrer-Mata, A., Sánchez-DelBarrio, J. C., Guirao-Rico, S., Librado, P., Ramos-Onsins, S. E., & Sánchez-Gracia, A. (2017). DnaSP 6: DNA sequence polymorphism analysis of large data sets. *Molecular Biology and Evolution*, 34, 3299–3302. <https://doi.org/10.1093/molbev/msx248>
- Schmidt, K. P., & Marx, H. (1956). The herpetology of Sinai. *Fieldiana Zoology*, 39, 21–40.
- Shacham, B., Federman, R., Lahav-Ginott, S., & Werner, Y. L. (2016). The northward extension of reptiles in the Palearctic, with the Jordan Valley (Israel) as a model: snakes outrace lizards. *Journal of Natural History*, 50, 1017–1033. <https://doi.org/10.1080/00222933.2015.1083057>
- Shacham, B., & Shifman, S. (1998). The *Tropicolotes* species in Israel is *T. nattereri*. *Israel Journal of Zoology*, 44, 88.
- Shifman, S., Shacham, B., & Werner, Y. (1999). *Tropicolotes nattereri* (Reptilia: Gekkonidae): comments on validity, variation and distribution. *Zoology in the Middle East*, 17, 51–66. <https://doi.org/10.1080/09397140.1999.10637768>
- Silvestro, D., & Michalak, I. (2012). raxmlGUI: a graphical front-end for RAXML. *Organisms Diversity and Evolution*, 12, 335–337. <https://doi.org/10.1007/s13127-011-0056-0>
- Sindaco, R., & Jeremcenko, V. K. (2008). *The reptiles of the Western Palearctic*. Edizioni Belvedere.
- Sindaco, R., Nincheri, R., & Lanza, B. (2014). Catalogue of Arabian reptiles in the collections of the “La Specola” Museum, Florence, *Scripta Herpetologica. Studies on Amphibians and Reptiles in Honour of Benedetto Lanza*, 3, 137–164.
- Stamatakis, A. (2006). RAxML-VI-HPC: maximum likelihood-based phylogenetic analyses with thousands of taxa and mixed models. *Bioinformatics*, 22, 2688–2690. <https://doi.org/10.1093/bioinformatics/btl446>
- Steindachner, F. (1901). Berichte der Commission für Oceanographische Forschungen. Expedition S. M. Schiff, “Pola” in das Rothe Meer nördliche und südliche Hälfte. 1895/96 und 1897/98. Zoologische Ergebnisse. XVII. Bericht über die herpetologischen Aufsammlungen. *Denkschriften Der Kaiserlichen Akademie Der Wissenschaften, Mathematisch-Naturwissenschaftliche Classe, Wien*, 69, 325–335.
- Stephens, M., & Donnelly, P. (2003). A comparison of Bayesian methods for haplotype reconstruction from population genotype data. *The American Journal of Human Genetics*, 73, 1162–1169. <https://doi.org/10.1086/379378>
- Stephens, M., Smith, N. J., & Donnelly, P. (2001). A new statistical method for haplotype reconstruction from population data. *The American Journal of Human Genetics*, 68, 978–989. <https://doi.org/10.1086/319501>
- Uetz, P., Slavenko, A., Meiri, S., & Heinicke, M. (2020). Gecko diversity: a history of global discovery. *Israel Journal of Ecology and Evolution*, 66, 117–125. <https://doi.org/10.1163/22244662-bja10003>
- Werner, Y. L. (1973). *The reptiles of the Sinai Peninsula*. Department of Zoology, Hebrew University.
- Werner, Y. L. (1988). Herpetofaunal survey of Israel (1950–85), with comments on Sinai and Jordan and on zoogeographical heterogeneity. *Monographiae Biologicae*, 62, 355–388.
- Werner, Y. L. (2016). *Reptile life in the land of Israel: with comments on adjacent regions, including a special photographic appendix by the publisher*. Edition Chimaira.
- Wilms, T. M., Shobrak, M., & Wagner, P. (2010). A new species of the genus *Tropicolotes* from Central Saudi Arabia (Reptilia: Sauria: Gekkonidae). *Bonn Zoological Bulletin*, 57, 275–280.

## SUPPORTING INFORMATION

Additional supporting information may be found in the online version of the article at the publisher's website.

**How to cite this article:** Ribeiro-Júnior, M. A., Tamar, K., Maza, E., Flecks, M., Wagner, P., Shacham, B., Calvo, M., Geniez, P., Crochet, P.-A., Koch, C., & Meiri, S. (2022). Taxonomic revision of the *Tropicolotes nattereri* (Squamata, Gekkonidae) species complex, with the description of a new species from Israel, Jordan and Saudi Arabia. *Zoologica Scripta*, 00, 1–22. <https://doi.org/10.1111/zsc.12532>